MODIFICATION AND COMMISSIONING OF A STATIC HIGH PRESSURE APPARATUS AND PHASE EQUILIBRIA MEASUREMENTS FOR FLUORINATED HYDROCARBONS

Submitted in fulfilment of the academic requirements for the degree of Master of Science,
Faculty of Engineering, School of Chemical Engineering,
University of KwaZulu-Natal
by

Kaleng Jim Chiyen

Supervisor: Prof. Deresh Ramjugernath
Co-Supervisor: Prof. Christophe Coquelet
Co-Supervisor: Dr. Prathieka Naidoo

May 2010

DECLARATION

I, Kaleng Jim Chiyen, declare that

I. The research reported in this thesis, except where otherwise indicated, is my original work.

II. This thesis has not been submitted for any degree or examination at any university.

III. This thesis does not contain other persons' data, pictures, graphs or other information, unless specifically acknowledged as being sourced from other persons.

IV. This thesis does not contain other persons' writing, unless specifically acknowledged as being sourced from other researchers. Where other written sources have been quoted, then:

   a) their words have been rewritten but the general information attributed to them has been referenced;

   b) where the exact words have been used, their writing has been placed inside quotation marks, and referenced.

V. Where I have reproduced a publication of which I am an author, co-author or editor, I indicated in detail which part of the publication was actually written by myself alone and have fully referenced such publications.

VI. This thesis does not contain texts, graphics or tables copied and pasted from internet, unless specifically acknowledged, and the source being detailed in the thesis and in the references sections.

_____ _____

Kaleng J. Chiyen (candidate) Date

As the candidate supervisor I agree/ do not agree to the submission of this thesis.

_____ _____

Prof. Deresh Ramjugernath Date

ABSTRACT

Modifications were undertaken to a static high pressure vapour-liquid equilibrium (VLE) apparatus described by Naidoo [2004]. The alterations were made to improve the sample analysis technique. These modifications included the incorporation of the ROLSI^{TM} sampling device into the equilibrium cell, a re-design of the air bath which improved the temperature profile and further alterations described in the text.

The equipment has an operating temperature range of 278.15 K to 473.15 K and pressure range of absolute vacuum to 150 bars. The apparatus consisted of an agitated cell in an air-bath. The uncertainties in the temperature and pressure measurements were ±0.02 K and ±4 kPa respectively. A Shimadzu Gas Chromatograph, Model 2010 was used for sample analysis.

An initial test of the apparatus was carried out to measure the pure component vapour pressure data for propane and ethane in the temperature range of 279.24 – 360.18K and the results concurred with literature data (absolute relative deviation <0.153%)

The experimental procedure used in this study was developed from the technique used by Ramjugernath [2000], with some minor changes implemented only to achieve some requirements for problems encountered during the project.

Isothermal binary measurements for the hexafluoroethane (R116) + propane system were used as test system to investigate the accuracy and reliability of the equipment. Three binary isotherms were measured at 291.22 K, 296.23 K and 308.21 K. The measured data compared well with literature data.

Particular attention was placed on the fluorinated hydrocarbons. Specific properties of fluorinated hydrocarbons give them many applications in industry, such as solvents, refrigerants, propellants, anaesthetics, etc. Hence, a phase equilibria study of a fluorinated hydrocarbons system was carried out in this project.

The commissioning of the equipment was successfully undertaken and the equipment was found to be efficient and reliable. As a consequence measurements were made on the hexafluoropropylene oxide (HFPO) + ethane system. No data has been previously published in literature for this system. Measurements were undertaken at five different temperatures, 283.15

K, 290.15 K, 298.15 K, 308.15 K and 318.15 K. The isotherms were chosen in order to have measurements below and above the critical temperature of ethane, in order to see the transition at the critical temperature.

The experimental data were modelled via the direct (phi-phi) method. The Peng-Robinson equation of state was applied, including the Mathias-Copeman alpha correlation with the Wong-Sandler mixing rules incorporating the NRTL activity coefficient model. Good agreement was found between the correlated and the measured data.

ACKNOWLEDGEMENTS

I would like to acknowledge the following people and organizations for their huge contribution to this work:

- My Lord and Saviour, Jesus Christ for his grace upon my life all along this project.

- My supervisors, Prof. Deresh Ramjugernath, Prof. Christophe Coquelet and Dr, Prathieka Naidoo for their tremendous support, guidance and ideas throughout this work.

- NRF for the financial support.

- My parents Alphonse Mukiny and Isabelle Kalong, my brothers and sisters for their love, assistance and motivation.

- The technical team, Lindinkosi Mkize, Ayanda Khanyile, Kelly Robertson, Les Henwood for their assistance on the equipement used in this work.

- All Thermodynamics Research Unit fellows, M. Tshibamgu, K. Tumba, J. Kapuku, F. Kabulo, X. Courtial, S. Iwarere, M. Tadie, W. Nelson, D. Lokhat,...

- All my church fellows, Pastor J. Tshosha, Pastor BB. Ezechiel, J. Tshimanga, T. Kalambay, S. Mapan, E. Beya, B. Sheshe, A. Kalumba,…

Table of Contents

LIST OF TABLES, FIGURES AND PHOTOGRAPH

Tables

Figures

Photographs

NOMENCLATURE

List of Symbols

a Parameter in cubic equations of state

B Second virial coefficient, density expansion

b Parameter in cubic equations of state

C Third virial coefficient, density expansion

D Fourth virial coefficient, density expansion

f Fugacity pure species (Pa)

$\hat{f}$ Fugacity species in solution (Pa)

G Gibbs energy ($J.mol^{-1}$)

ΔH Enthalpy change of mixing (J)

K_i Vapour liquid equilibrium ratio for species i

k_{ij} Binary interaction parameter in EOS

n_i Number of moles of species i

P Absolute pressure (Pa)

P_c Critical pressure (Pa)

R Universal Gas constant ($J\ mol^{-1}\ K^{-1}$)

T Absolute temperature (K)

V Molar or specific volume (m^3)

x Mole fraction of species in liquid phase

y Mole fraction of species in vapour phase

Z Compressibility factor

Superscripts

E Excess thermodynamic properties

id Ideal solution

ig Ideal gas

L Liquid phase

R Residual thermodynamic properties

V Vapour phase

∞ Infinite dilution

Λ Thermodynamic properties in solution

- Partial properties

o Standard-state

Greek letters

α Function in cubic equations of state

β Parameter in cubic equation of state

γ Activity coefficient for species in solution

μ Chemical potential

τ Temperature ratio

Φ Ratio of fugacity coefficients

ϕ Fugacity coefficient for pure species

ω Acentric factor

Subscripts

i Properties related to pure component i

ij Interaction properties

c Critical Properties

r Reduced Properties

m mixing properties

Overbars

- Partial molar property

^ Property of component in a mixture

CHAPTER 1: INTRODUCTION

Separations, including enrichment, concentration, purification, refining, and isolation, are important to chemical engineers (Seader and Henley, 1998). Separation processes account for a significant percentage of the average chemical plant; they account for more than 50% of total capital costs and 90% of total energy usage. Purposes for which separation techniques are used include extraction of metals from ores and perfumes from flowers, the evaporation of seawater to obtain salt, the distillation of liquors and many others. Separation equipment is designed mainly on the basis of thermodynamic equilibrium. As a result the measurement and modelling of vapour liquid equilibrium plays a considerable role in chemical process design.

The Thermodynamic Research Unit in the School of Chemical Engineering at the University of KwaZulu-Natal has a reputation as a productive centre for phase equilibria studies, and is known as one of the best in Africa and in the Southern Hemisphere. The unit has been producing VLE data for more than twenty-five years, data which has assisted many local companies to improve their separation processes.

A piece of static high pressure vapour-liquid equilibrium (HPVLE) apparatus was designed in the unit for the measurement of HPVLE data. Recommendations from other researchers who had used the apparatus were taken into consideration to improve the efficiency of the apparatus. Some of those recommendations dealt with the complexity of the sampling method and the length of time taken to reach equilibrium.

Fluorinated hydrocarbons have recently gained importance in industry. The relatively low reactivity, low critical temperature, low surface tension, excellent dielectric properties and high polarity that result from the carbon-fluorine bond give them their particular characteristics. As a result of these characteristics, they have found applications in various fields, some of which are described below.

Since the Montreal Protocol in 1987, refrigeration processes have been required to use new refrigerant fluids to replace the ozone-destroying components. An alternative was found in fluorinated hydrocarbons, such as difluoromethane, trifluoromethane, tetrafluoromethane, hexafluoroethane, etc.

Two tasks were assigned in this work. Firstly modifying the existing static HPVLE apparatus in order to resolve the problem cited previously, and so improve the efficiency and functionality of the equipment.

The second aim was to perform vapour-liquid equilibrium (VLE) measurements of a few systems containing fluorinated hydrocarbons. This was in order to determine their phase equilibrium behaviour while mixed with different components for developing further applications in industry.

Hexafluoropropylene oxide (HFPO) is a multipurpose fluorocarbon. Its uses include the synthesis of various fluoromonomers and fluoropolymers. It also can be used in the refrigeration industry and in many other applications. Hence VLE measurements were performed specifically on the HFPO + Ethane system to determine its behaviour in mixture with hydrocarbons. Measurements undertaken in this work are part of a project on refrigerant conducted by the Thermodynamic Research Unit and the Mines Paris Tech in Fontainebleau (France).

In addition the measured data will help in the development of group contribution methods, which are methods for the prediction of thermodynamic properties from molecular structures. HFPO has two functional groups, the fluoro and the epoxide functions, which have not yet been described by contribution methods.

South Africa has one of the largest fluorspar reserves in the world, but there is a limit beneficiation of the ore. The Department of Science and Technology (DST) through the South African Research Chair of Fluorine Process Engineering and Separation Technology has initiated numerous projects to maximise the revenue of the country from the fluorochemicals market by beneficiation of the fluorspar. This work is one of the projects initiated for this purpose.

In this project, HPVLE were measured at moderate temperatures for a binary system with data available in literature as well as for a system with previously unpublished data. Measured binary VLE data, already available in literature were used to check the efficiency of the modified equipment and the experimental technique.

CHAPTER 2: FLUORINATED HYDROCARBONS

2.1 Introduction

Fluorinated hydrocarbon refers to any organic compound containing carbon and fluorine combined in strong carbon-fluorine bonds. They have a unique position among fluorinated compounds because of their special properties. The nomenclature of fluorinated hydrocarbons is presented in Appendix A.

Regular studies of fluorinated hydrocarbons started in 1937 with Simons and Block, when they discovered a way to carry out the reaction between fluorine and carbon by impregnating the carbon with mercury salt. From 1940 forward, the fluorinated hydrocarbons industry has experienced significant development as a result of the implementation of different synthesis methods (Emeleus, 1969).

2.2 Properties of Fluorinated Hydrocarbons

Fluorinated hydrocarbons are dissimilar in certain ways to other halocarbons; this is due to three main factors as described by Kirk-Othmer [1966]. These factors are the high electronegativity of fluorine (3.98 on the Pauling scale), the relatively small size of fluorine (1.35 Å) which gives it the capacity to replace even hydrogen atoms in a compound without excessive steric strain, and the last which pertains to the presence of unpaired electrons.

2.2.1 Physical properties

A huge discrepancy was found between the physical properties of fluorinated hydrocarbons and the corresponding hydrocarbons. The physical properties are also greatly affected by the number of carbon atoms in the molecule. The higher the number of carbon atoms in the molecule, the higher the density, critical properties, boiling point, viscosity, surface tension and vapour-pressure.

Liquid fluorinated hydrocarbons have similar viscosities to those of other hydrocarbons, but these viscosities appear low when compared to liquids of similar boiling points. This is due to the relatively weak intermolecular forces. They are colourless and have high densities, generally twice that of water due to the high molecular weight. Fluorocarbons have a low toxicity, low surface tension and good dielectric properties.

For a liquid to wet a solid, the surface tension of the liquid must be lower than that of the solid. Solid fluorinated hydrocarbons are the best non-wettable and non-adhesive surfaces known as a result of their low surface tension. Among fluorinated hydrocarbons perfluoromethyl ($-CF_3$) is the best non-adhesive substance.

Fluorinated hydrocarbons compounds are very stable, especially those with a single bond. O'Hagan [2008] explained this stability by the strength and the nature of the carbon-fluorine bond. This bond is rated the strongest bond in organic chemistry. Lemal [2004] established that the presence of multiple carbon-fluorine bonds increases the stability of the entire molecule. Consequently fluorinated hydrocarbons compounds are thermally stable.

2.2.2 Chemical properties

Fluorinated hydrocarbons have significant chemical stability. They do not react easily even at high temperature and are not attacked by acids and oxidizing agents. The greater the number of carbon atoms in the molecule, the less chemically stable the molecule is.

As stated previously. The presence of the carbon-fluorine bond gives stability to the fluorocarbon compound, and this is not only thermally but also chemically stable. However fluoroalkenes and fluoroalkynes are less stable than saturated fluorocarbons. Kiplinger et al. [1994] reported reactions through nucleophiles and hydrolysis in solution.

2.3 Fluorinated Hydrocarbons and the environmental aspect

2.3.1 Ozone Depletion Potential (ODP)

The ODP is the ability that a compound has to contribute to the degradation of the stratospheric ozone layer. The ODP can be estimated from the structure of the substance. Table 2-1 gives examples of ODPs for some chemicals.

Table 2-1: ODPs values for some chemicals extracted from Scientific Assessment of Ozone-Depletion (SAOD) (2006)

CHEMICAL	ODP	TIME HORIZON (Years)
Trichlorofluoromethane (R11)	1.0	45
Brominated substances	From 5 to 15	65

CHEMICAL	ODP	TIME HORIZON (Years)
Hydrochlorofluorocarbons	From 0.005 to 0.2	-
Fluorinated hydrocarbons	0	-

The fluorine atom does not react with ozone.

The Montreal Protocol was signed on the 16th September 1987, with the aim of protecting the ozone layer by limiting the use of certain substances thought to cause ozone depletion. Since its inception the protocol has been adopted all over the world. Due to the Montreal Protocol some of the designated chemicals, especially refrigerants have been banned, and attention is shifting to the ozone friendly substances, such as fluorinated hydrocarbons.

2.3.2 Global Warming Potential (GWP)

The GWP is the measure of the ability that a greenhouse gas has to contribute to global warming, compared to the ability of carbon dioxide. The GWP is determined by the atmospheric lifetime and the radiation characteristics of the gas. The following table represents the GWP values of some fluorinated hydrocarbons.

Table 2-2: The GWP values and the lifetime of some fluorinated hydrocarbons. The first value in the second and third columns is from Scientific Assessment of Ozone-Depletion (SAOD) (2002); and the second and third values are from the Intergovernmental Panel on Climate Change (IPCC) (2001).

CHEMICAL	LIFETIME / years	GWP
CO_2 (R744)	All time periods	1
CHF_3 (R23)	270	12240
	264	11700
	260	12000
CH_2F_2 (R32)	4.9	543
	5.6	650
	5.0	550

CHEMICAL	LIFETIME / years	GWP
CH_3F (R41)	2.4 3.7 2.6	90 150 97
C_2F_6 (R116)	10000 10000 10000	12010 9200 11900
C_3F_8 (R218)	2600 2600 2600	8690 7000 8600
C_4F_{10} (R610)	2600 2600 2600	8710 7000 8600

It is evident that fluorocarbons have a higher greenhouse potential compared to carbon dioxide.

2.4 Uses

Fluorinated hydrocarbons have recently gained importance in industry. The relative low reactivity, low critical temperature and high polarity resulting from the carbon-fluorine bond give them particular characteristics. The need for new fluids as refrigerants to replace the ozone-destroying component, since the Montreal Protocol, made them more important in industry. Some uses of fluorinated hydrocarbons are provided below.

2.4.1 Refrigerant

Refrigeration has applications ranging from cooling food in supermarkets to cooling buildings with air-conditioners to promoting industrial safety and efficiency through coolant reactors in chemical plants and many others. Refrigeration technology has evolved over time from the

simple use of ice to cool food through the use of various substances that absorb head though expansion and/or vapourisation.

2.4.1.1 Evolution of Refrigerants

Calm [2008] traced the evolution of refrigerants in four generations.

First Generation: The first generation used any chemicals that could work and were available. Most of these refrigerants were toxic, flammable or both. Accidents were frequent. Refrigerants such as propane, ammonia and carbon dioxide were very popular.

Second Generation: The second generation moved to fluorochemicals, which were durable and in most of the cases safe. Chlorofluorocarbons dominated the second generation. Midgley [1937] detailed eight elements that constitute the refrigerants of the second generation; these are carbon, nitrogen, oxygen, sulphur, hydrogen, fluorine, chlorine, and bromine. The refrigerants of the second generation remained flammable and toxic.

Third Generation: The third generation shifted to components friendly to the ozone layer. Fluorochemicals kept the main place. Some natural refrigerants such as ammonia, carbon dioxide, hydrocarbons were investigated.

Fourth Generation: The fourth generation refrigeration technology combines concerns about the ozone depletion and the global warming characteristics of refrigerants. Therefore, for a component to be used as a refrigerant, aside being able to produce cold and being durable, it must not have a destructive effect on the ozone layer and must not be a greenhouse gas.

Ananthanarayanan [1992] establishes some desirable properties for a refrigerant, such as high critical temperature and pressure, low freezing point, low boiling point, stability, non-toxic, non-explosive, non-flammable, chemical inertness and non-ozone depleting.

Most of fluorinated hydrocarbons, especially those with relatively high numbers of carbon atoms meet most of the required properties for refrigeration. Thus fluorinated hydrocarbons see significant use in the refrigeration industry.

2.4.2 Solvents

Many fluorocarbons are used as solvents in industry, due to their possessing properties such as stability, excellent dielectric properties, low surface tension and viscosity, low toxicity, low

boiling point. It is well known that solvents play a major role in modern industrial society. Most reactions are carried in the liquid phase. The following are some details about properties that give fluorocarbons the ability to be used as organic solvents:

- Excellent dielectric properties: Polar solvents dissolve polar compounds and non-polar solvents dissolve non-polar compounds. Tinoco [2008] stated that the solvent with a small dielectric constant will be non-polar, thus good for non-polar reactants. Fluorocarbons have dielectric constants around 6.4, which is relatively low and make them adequate for dissolving non-polar reactants.

- Low surface tension: surface tension is a property of a liquid that determines the surface portion of a liquid to be attracted by another surface. According to Durkee [2002] a high surface tension is resistant to the attraction; on the contrary a liquid with a low surface tension will have a good attraction with another liquid. Fluorocarbons have relatively low surface tension; therefore they manifest a good attraction on contact with another surface.

- Viscosity: Lewandowski [2006] classified fluorocarbon components as low viscosity fluids; this explains their ability to dissolve so many organic reagents.

- Low Toxicity: As quoted previously most fluorocarbons are not toxic; this enables them to be used safely.

2.4. 3 Semiconductor

Organic materials play a major role in electronic industry; semiconductors are mostly made with organic compounds and silicon, because of their potential in switches and modulators. 1, 1-dichloro-1-fluoroethane is widely needed in the manufacture of electronics. Unfortunately, it has a destructive action on the ozone layer (ODP=0.11) and its use has therefore been restricted. Fluorinated hydrocarbons can be used as substitute solvents.

The McClean Report [2009] stated that the worldwide semiconductor market has encountered a major boom since 2000 and has reached US$ 318 billion/annum. The same report predicts that the market will reach $ US 400 billion in the few coming years. This will imply great revenue for the fluorocarbon market, as they constitute one of the major components in the manufacture of semiconductors.

2.4.4 Propellant

A propellant is any material which by its reaction creates movement of an object. A propellant can be a solid, liquid, gas or plasma. According to a study led by NASA in 1958 [www.history.nasa.gov/conghand/propelnt.html], an efficient propellant must have a high heat of combustion, a high density, light combustion products and be safely practical.

Although fluorinated hydrocarbons do not have high heats of combustion, they have high density as stated by Lemal [2004], and are non-toxic and non-flammable, and they release very simple molecules after combustion. It is for these reasons they are frequently use as propellants.

The list of the uses for fluorinated hydrocarbons is not exhaustive; many of their applications are not mentioned in the text, only those which have been considered important were described. Fluorinated hydrocarbons are also used as anaesthetics, storage agents for biological specimens, surfactants, cleansing and protecting agent in cosmetics, blowing agent for foams, and in many other industries.

CHAPTER 3: REVIEW OF HIGH PRESSURE VAPOUR-LIQUID EQUILIBRIUM EQUIPMENT

3.1 Classification of experimental methods

Deiters and Schneider [1986] classified systems of high-pressure phase equilibrium experimental methods and established the synthetic and the analytic methods. The analytic method is characterized by the analysis of one or both phases, liquid or/and vapour; while the synthetic method is one in which a sample of known composition is charged into the equilibrium cell and its behaviour is observed according to the pressure and the temperature of the system.

A detailed and clear classification has been compiled by Raal and Mühlbauer [1998]. The classification depends on the circulation or lack of circulation of the phases. When the phases are in circulation the method is called dynamic and when none of the phases is in circulation the method is static. Sometimes, both methods are combined, and then the method is called dynamic-static.
Below is the diagram showing these classifications:

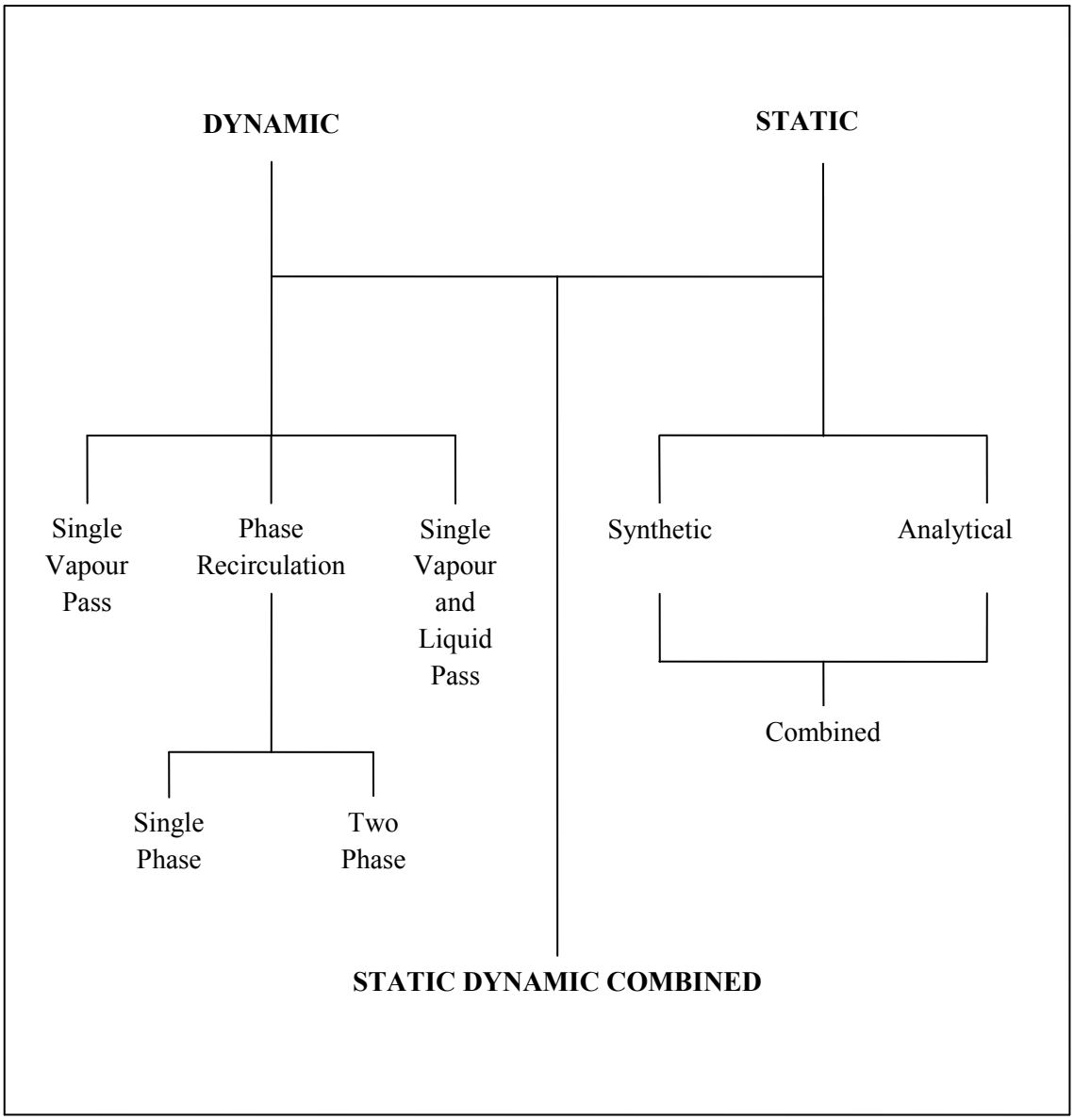

Figure 3-1: Classification of high-pressure vapour-liquid equilibrium methods (from Raal and Mühlbauer, 1998).

3.2 Principal features of HPVLE experimental equipment

The principal features of any experimental HPVLE apparatus are listed below from the work of Raal and Mühlbauer [1998]:

- An equilibrium cell in which the vapour and liquid phases are in equilibrium with each other.

- An environment for the control of the temperature of the equilibrium cell. The equilibrium cell is located in this environment which, in most cases, is a bath filled with a fluid in circulation (air, nitrogen, water, alcohol, etc).

- A mechanism of agitation to increase the rate of equilibration. The static method uses an internal stirrer whilst in the dynamic method the circulation of the phases provides sufficient agitation.

- The analytical method requires a method of analyzing both liquid and vapour phases. This can be satisfied by an external device such as a Gas Chromatograph (GC). It also requires removing a representative sample. Sometimes analyses are performed in-situ by means of an optical device.

- The synthetic method requires a means of adjusting the equilibrium cell pressure and temperature. It is usually achieved by adjustment of the cell volume, to bring about phase separation.

- Devices for measurement of pressure and temperature.

- Insulation is necessary when working at temperatures different from ambient.

3.3 Challenges encountered during HPVLE experimentation

This section below is based on the work of Raal and Mühlbauer [1998].
Difficulties expected in attaining accurate measurement of HPVLE include the following:

- Degassing of liquid components before entering into equilibrium cell.
- Attaining of true isothermal equilibrium conditions.
- Establishing that equilibrium has been reached.
- Measuring of accurate temperature and pressure of the equilibrium cell.
- Sampling of the liquid and vapour phase without disturbing the equilibrium condition.
- Preparation of truly representative sample for analysis.
- Accurately analyzing the withdrawn samples.

3.3.1 Degassing of liquid components at the start of experimentation

It is necessary to remove all dissolved gases from the liquid component, since the presence of the gas in the liquid can affect the adsorption of the volatile component into the liquid component. It also introduces error into the values of pure component vapour-pressures. Degassing becomes more important in systems dealing with two components slightly soluble in one another. The liquid component can be degassed in-situ in the equilibrium cell or before introducing it in the cell by the use of appropriate equipment.

3.3.2 Obtaining true isothermal equilibrium conditions

The temperature gradients in the equilibrium cell must be as small as possible in order to get the true equilibrium conditions at the set temperature. Inducing isothermal conditions in the equilibrium cell is difficult when it comes to volatile/non-volatile component systems. Care should be taken with these systems to avoid certain problems when sampling. Therefore any heat conduction via conductive lines linked to the cell and any direct radiation energy exchange between the cell and the bath heaters should be avoided. More than one sensor should be installed in the walls of the cell to check that temperature is constant; according to Raal and Mühlbauer [1998] the acceptable temperature gradient is 0.5 K or less.

3.3.3 Establishing the Attainment of equilibrium

Thermodynamic equilibrium involves no change in the properties and quantity of material occuring over time. In other words, thermodynamic equilibrium implies a balance of all potentials that lead to change. High stirring increases the contact between different phases, hence it decreases the time needed to reach equilibrium. The rate of change decreases while approaching equilibrium. A true state of equilibrium is impossible due to continual transformation in the system. As a result, equilibrium is assumed when changes are no longer detected by the measuring devices. Some properties such as temperature, pressure, vapour and liquid composition are determinant factors in establishing the equilibrium. Various authors give values in some variables at which they assume equilibrium; Fredenslund et al. [1973] set a change in the pressure of less than 0.05% within half an hour to assume the equilibrium.

3.3.4 Temperature and pressure measurement

Various instruments can be used for temperature measurement. Thermocouples are preferable for temperatures above 423.15 K. Platinum resistance thermometers seem to be the preferred devices for experimentation between 0 and 373.15 K.

For pressure measurement, bourdon pressure gauges and electronic pressure transducers are used.

3.3.5 Avoiding disturbance of equilibrium during sampling

During the sampling process, a quantity of material is withdrawn from the system. The larger the volume removed, the greater the disturbance of equilibrium. This change in volume is evaluated based on pressure change. Pressure fluctuations of 10 and 1 kPa have been reported by Besser and Robinson [1971] and Wagner and Wichterle [1987], respectively. The withdrawn sample volume is influenced by two factors; the volume of the sample and the sampling method. The size of the sample taken from the cell is fixed mainly by the analytical device whereas the method of sampling must lead to the lowest possible volume change in the cell. As stated by Sagara et al. [1972], Klink et al. [1975], Aschroft et al. [1983], Reiff et al. [1987] and Mühlbauer [1990], to overcome the volume change problem, one should use a large equilibrium cell volume. However this method has the disadvantage of increasing the quantity of chemicals required for the measurements.

To minimize the risk of disturbing the equilibrium during sampling, the task is to implement an appropriate sampling method with characteristics as reported below:

- A rapid sampling method in order to shorten the time for risk of equilibrium changes as stated by Figuiere et al. [1980].

- A sampling method where the volume change is only caused by the withdrawn sample.

- A sampling method where volume change can be balanced by pressure adjustment, Nakayama et al., [1987].

- Using optical methods if possible, for in-situ analysis of the equilibrium cell contents without removing any samples.

3.3.6 Preparation of withdrawn sample for analysis

Karla et al. [1978] noted that there is a tendency for the volatile component to flash preferentially when sampling the liquid phase of a volatile/non-volatile system. The challenge will be to implement a method of taking homogenized samples, hence avoiding flashing of the volatile component and condensation of the non-volatile component. One of the difficult tasks is to homogenize the vapour mixture without re-condensation of one of the components. Below are some actions recommended to re-homogenize and prevent partial condensation of the liquid samples:

- Wagner and Wichterle [1987] used a stirred homogenization vessel in the sample line.

- Kobayashi and Katz [1953], Rogers and Prausnitz [1970], Simnick et al. [1977], and Inomata et al. [1986] analyzed the volatile component and non-volatile component separately. The method in this case consists of separating the volatile from the non-volatile component in a sample using an evacuated vessel. The condensed non-volatile components were flushed out of the vessel with an organic solvent. The calibration standard was added and the final mixture analyzed using the gas chromatograph.

- Kalra et al. [1978], Ng and Robinson [1978], and Nakayama et al. [1987] set the sampling lines at the equilibrium temperature and used the circulation system to rehomogenize the sample before sending it to the gas chromatograph.

- Heating of all the lines carrying samples to the gas chromatograph to a temperature higher than the equilibrium temperature and keeping the pressure in the lines low to avoid condensation. The temperatures recommended are 50 to100 K higher than the equilibrium temperature.

- Ejection of the liquid sample in the jet mixer at a temperature 50 K higher than the equilibrium temperature. The jet mixer leads to the vaporization of the sample and the vapour produced is homogenized by the use of a swirling recirculation motion within the mixer.

3.3.7 Accurate analysis of the vapour and liquid phases

Two primary methods are used for the analysis of vapour and liquid phase samples, viz. gas chromatography and spectroscopy for external analysis and in-situ analysis respectively. Besserer and Robinson [1971] and Kalra et al. [1978] have, however, also reported the combination of refractive index measurements with gas chromatography.

Gas chromatography: This instrument uses a thermal conductivity detector (TCD), which is used to detect hydrocarbons and non-hydrocarbons or a flame ionization detector (FID), which detects organic components only. Below are some disadvantages of the gas chromatograph:

- While working at high-pressure or/and high temperature, the state of the sample entering the GC is different from the equilibrium state.

- Producing accurate calibration of the detector while working with gas mixtures is difficult. For most cases the response-factor ratio changes with the concentration.

Spectroscopic method: This method was proposed to overcome difficulties associated with the preparation of the sample for the GC. A spectroscopic method is performed in-situ. Use of infrared spectra to determine a phase concentration has been reported by Swaid [1984], where the absorption bands are often well separated. Below are some disadvantages of the infrared, visual, and ultraviolet spectroscopy or Raman scattering methods:

- Only aromatic or coloured compounds can be analyzed using the ultraviolet or visual spectroscopy.

- Extensive calibration procedures are required compared with those required for gas chromatography.

- There is a risk of overlapping absorption bands of different components with infrared spectroscopy.

Table 3-1: Review of HPVLE static equipments

Authors	Equilibrium cell		Temp range [K]	Press range [MPa]	Measurement device		Sampling device	
	Material of construction	Volume [cm^3]			Temp	Pressure	Liquid	Vapour
Rogers and Prausnitz [1970]	Stainless steel	150	223.15 – 423.15	100	TC	Floating piston gauge + strain gauge	Set of moving piston	Set of moving piston
Besserer and Robinson [1971]	Stainless Steel	From 10 to 175	223.15 – 423.15	100	TC	Pressure transducer	Sampling valve	Sampling valve
Kalra and Robinson [1975]	316 Stainless steel	250	173.15 – 339.15	35	TC	Pressure transducer	Needle valve	Needle valve
Ng and Robinson [1978]	316 Stainless steel + Pyrex glass window	150	310.85 – 588.15	17.2	TC	Pressure gauge	Sampling rod	Needle valve
Figuiere et al. [1980]	Stainless steel	50	423.15 – 673.15	40	TC	Pressure transducer	Valves that were opened by a hammer	Valves that were opened by a hammer

Table 3-1 (Continued): Review of HPVLE static equipments

Authors	Equilibrium cell		Temp range [K]	Press range [MPa]	Measurement device		Sampling device	
	Material of construction	Volume [cm^3]			Temp	Pressure	Liquid	Vapour
Bae et al. [1981]	304 stainless steel + glass window	300	223.15 - 323.15	10	PRT	Pressure transducer	Sampling rod	Sample expansion
Ashcroft et al [1983]	Manganese steel + glass window	885	298.15 – 330	69	Thermistor	Pressure transducer	Sampling rod	Capillary sampling
Guillevic et al. [1983]	316 Stainless steel	50	558	7	TC	Pressure transducer	Capillary microvalve	Capillary microvalve
Laugier & Richon [1983]	316 stainless steel	50	423	10	TC	Pressure transducer	Capillary	Capillary
Wagner and Wichterle [1987]	Stainless steel + two pyrex glass windows	65	303-323	10	QT	Bourdon gauge	Capillary + a six-way valve	Capillary

Table 3-1 (Continued): Review of HPVLE static equipments

Authors	Equilibrium cell		Temp range [K]	Press range [MPa]	Measurement device		Sampling device	
	Material of construction	Volume [cm^3]			Temp	Pressure	Liquid	Vapour
Mühlbauer [1990]	316 Stainless steel	350	453	20	PRT	Pressure transducer	Sampling rod	Sampling capillary
Zabaloy et al. [1993]	Brass + glass disks	50	298.15 – 370	4.1	Thermistor	Pressure transducer	Sampling valves	Sampling valves
Kang & Lee [1996]	316 Stainless steel	545	323	0.7	TC	Pressure gauge	No Liquid analysis	-
Baba-Ahmed et al. [1999]	Hastelloy C276	43	<70	40	PRT	Pressure transducer	Pneumatic capillary	Pneumatic capillary
Valtz et al. [2002]	316 Stainless steel + sapphire window	30	223.15 - 473.15	10	Pt-100	Pressure transducer	ROLSI™ sampler	ROLSI™ sampler

PRT: Pressure resistance thermometer; QT: Quartz thermometer; TC: Thermocouple

A more detailed review of HPVLE static equipment is presented in the work of R. Dohrn and G. Brunner [1995]. In this chapter, equipment was selected with the intention of showing the evolution of sampling technique, as this is the main modification of the equipment used in this project. The sampling technique evolved from a complex set of moving piston to a simple capillary activated electrically. All along the development of the HPVLE static apparatus, difficulties were encountered with various sampling techniques used. Below, some of these difficulties are detailed, which difficulties were the cause of moving from one technique to another.

- **Set of moving piston:** This technique was used in the apparatus of Rogers and Prausnitz [1970], the sample technique consisted of removing sample from the equilibrium cell by the means of two set of moving pistons attached to the cell. The set of pistons is comprised with two pistons separated by a variable volume cavity. At the sampling time this volume moved until the sample ports are reached. The sample is then withdrawn from the cell. This technique presented the risk of pressure change. It required the use of special O-ring seals and heavy duty Teflon material. There was also a risk of mixing the vapour and the liquid phase.

- **Sampling valve:** The apparatus of Besserer and Robinson [1971] and of Zabaloy et al. [1993] used this sample technique. The method was simple and consisted of using micrometering valves, which, allowed the removal of sample from the cell by flushing. The average size of withdrawn sample was given by Besserer and Robinson [1971] as 10^{-3} g-mol, 0.2% depletion in terms of the overall cell volume. This is not negligible considering if one must take at least four samples to ensure reliably replicated data.

- **Needle valve:** The needle valves were used in the apparatus of Kalra and Robinson [1975] and Ng and Robinson [1978]. The needle valves were incorporated to the wall of the cell. The needle valve was connected to a manifold, which received the sample and sent it to the analysis instrument. A flow of helium gas supplied externally helped to carry the sample. The method failed to give representative sample of volatile/non-volatile system, as the lighter component tended to flush preferentially with respect to heavier component.

- **Sampling rod:** This technique was used in the apparatus of Ng and Robinson [1978], Bae et al. [1981], Ashcroft et al [1983] and Mühlbauer [1990]. The sampling tool was

a 5 mm diameter rod immersed in the liquid phase. The rod was drilled with a hole of approximately 3.5 µl. This hole was filled with liquid sample, and by the means of a piston moved from the liquid phase out of the cell. Helium gas was used to carry the sample from the rod to the analysis instrument. The method was able to produce good results, unless the time taken for sampling was unsatisfactory.

- **Valves that were opened by a hammer:** The apparatus of Figuiere et al. [1980] used sampling valves that were opened by hammer activated by an electromagnet. The problem with this method is that it was reliant on the opening time of the valves. This technique was found heavy and insufficiently trustworthy.

- **Pneumatic capillary:** The apparatus of Baba-Ahmed et al. [1999] used this technique. The method consisted of a capillary one end of which was immersed in the cell, with the other end in a chamber receiving the carrier gas going to the GC. The capillary was blocked off by a point activated by pressurized air. The opening and closing of the capillary was achieved by the pneumatic point. Samples of 1 to 5 micro litres were taken. The method was practical and led to good results.

- **Rapid Online Sampler Injector (ROLSI^{TM}):** Valtz et al. [2002] used this method. This technique was similar to that of the pneumatic capillary, the only difference was that the ROLSI^{TM} was activated electronically, which rendered its use easier and more precise. More details about the ROLSI^{TM} are provided in chapter V.

CHAPTER 4: THEORETICAL ASPECTS OF HIGH-PRESSURE PHASE EQUILIBRIUM

There are many possible liquid and vapour mixtures and it is almost impossible to produce VLE data for all such systems. Moreover, the process of obtaining good experimental data is difficult and expensive; it requires good experimental skill, knowledge, patience and experience. Thus the need to make some predictions of the experimental data based on correlations with similar systems arises, in order to determine the system behaviour at various conditions.

Thermodynamic theory provides the framework for data correlation or prediction. This theory is commonly applied at low pressure, however when applied to mixtures at high pressures, the task become more difficult. This is due to the introduction of non-ideality in the system for the high pressure. However, with the application of powerful software, the task is less complicated. Generally, there are two categories of theoretical methods for data correlation:

1. The direct method, known commonly as phi-phi method and
2. The combined method, known commonly as gamma-phi method

For the direct method, the fugacity coefficients of both liquid and vapour phases are computed via an Equation of State (EOS). For the combined method, the liquid phase activity coefficient is computed via a liquid phase activity coefficient model and the vapour phase fugacity coefficient via an EOS.

4.1 Criterion for phase equilibria

According to Van Ness et al. [2005] phase equilibrium is a static condition in which no changes occur in the macroscopic properties of a system over time. Equilibrium is also defined as the state when all potentials susceptible to change are equal for different phases. The criterion of thermodynamic equilibrium in binary vapour-liquid equilibrium is defined by the state at the same temperature, pressure and chemical potential or fugacity in both phases.

$$\hat{f}^{L}{}_{i}(T,P,x_i) = \hat{f}^{V}{}_{i}(T,P,y_i) \tag{4.1}$$

$\hat{f}_i$: is the fugacity of the component i in solution.

V and L : are the vapour and liquid phases respectively.

Prausnitz et al. [1980] proposed an expression for the fugacity that is produced from the first principle based on to the three most commonly measured variables, temperature, pressure and composition.

$$d\ln\hat{f}_i = \left(\frac{\partial \ln \hat{f}_i}{\partial T}\right)_{P,x} dT + \left(\frac{\partial \ln \hat{f}_i}{\partial P}\right)_{T,x} dP + \sum_{j=1}^{n-1}\left(\frac{\partial \ln \hat{f}_i}{\partial x_j}\right)_{P,T,x_k} dx_j \tag{4.2}$$

The right-hand-side terms of the equation are very complex, this makes the equation unusable. So, it requires relating the fugacity to measurable variables, such as temperature, pressure and phase compositions through the use of secondary functions such as the activity coefficient γ and the fugacity coefficient ϕ.

4.2 The direct method

As quoted previously, the direct method describes the fugacity coefficients of both the liquid and vapour phases by the use of an equation of state.

$$\hat{f}_i^L = x_i \hat{\phi}_i^L P \tag{4.3}$$

$$\hat{f}_i^V = y_i \hat{\phi}_i^V P \tag{4.4}$$

x_i and y_i are respectively the mole fractions of component in the liquid and vapour phases, and $\hat{\phi}_i^L$, $\hat{\phi}_i^V$ are the fugacity coefficients of component i in the liquid and vapour phases, respectively, according to the equilibrium condition. These equations may be written as:

$$x_i \hat{\phi}_i^L = y_i \hat{\phi}_i^V \tag{4.5}$$

The two fugacity coefficients are calculated using an appropriate EOS and an exact thermodynamic relationship.

For the vapour phase:

$$\ln \hat{\phi}_i^V = \left(\frac{1}{RT}\right)\int_{V^V}^{\infty}\left[\left(\frac{dP}{dn_i}\right)_{(T,V,n_j)} - \frac{RT}{V^V}\right]dV - \ln\left[\frac{PV^V}{n_T RT}\right] \tag{4.6}$$

For the liquid phase:

$$\ln \hat{\phi}_i^L = \left(\frac{1}{RT}\right)\int_{V^L}^{\infty}\left[\left(\frac{dP}{dn_i}\right)_{(T,V,n_j)} - \frac{RT}{V^L}\right]dV - \ln\left[\frac{PV^L}{n_T RT}\right] \tag{4.7}$$

As stated by Raal and Mühlbauer [1998] the use of the direct method at high pressure becomes complicated as:

- Vapour phase non-idealities become prominent.
- The total pressure differential term in the isothermal Gibbs-Duhem equations becomes important.

4.2.1 Problems related to the application of the direct method

Raal and Mühlbauer [1998] noted some difficulties encountered in application of the direct method:

- The selection of the most suitable EOS to describe both liquid and vapour phase non-idealities is a challenge as there are in literature, hundreds of EOS. The main criterion in this selection is that the EOS must be flexible enough to fully describe a pure substance P,V and T behaviour for both phases in the temperature and pressure range under study.

- Selecting the appropriate mixing rules. The mixing rules extend the pure component form of the EOS to mixtures. Most mixing rules are empirical and tend to be specific to the system.

- The problem of locating the suitable liquid and vapour molar densities when higher than cubic equations of state are used.

The block diagram (Figure 4.1) represents the computational scheme for the calculation of $x_i$and y_i from the experimental data P and T in direct method.

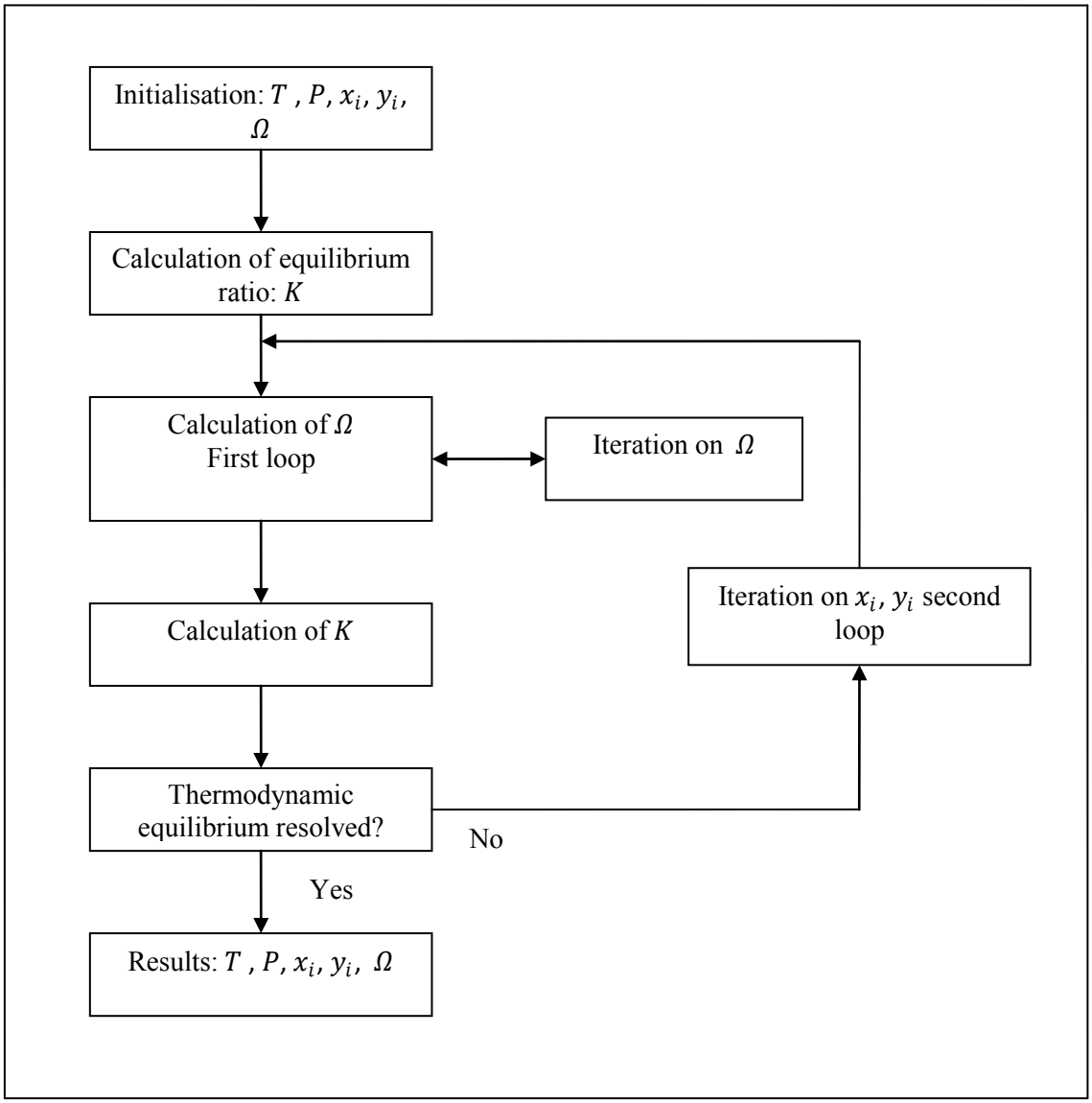

Figure 4-1: Block diagram for the flash calculation from isothermal vapour-liquid equilibrium used in Thermopack™ Software.

Where Ω is the rate of vaporisation, which is defined by the following expression:

$$\Omega = \frac{V}{L+V} \tag{4.8}$$

With V and L representing the mass of vapour and liquid respectively.
And the equilibration ratio is obtained by this formula:

$$K = \frac{y_i}{x_i} \tag{4.9}$$

4.3 The combined method

The basis of this method is the use of separate secondary functions to describe the non-ideality of both phases.

For the vapour phase:

$$\hat{f}_i^V = y_i \hat{\phi}_i^V P \tag{4.10}$$

For the liquid phase:

$$\hat{f}_i^L = x_i \gamma_i f_i^{OL} \tag{4.11}$$

Therefore at equilibrium

$$y_i \hat{\varphi}_i^V P = x_i \gamma_i f_i^{OL}(T,P) \tag{4.12}$$

As in the direct method the vapour phase is calculated using a suitable EOS through the exact thermodynamic relationship:

$$\ln \hat{\phi}^{V}{}_{i} = \left(\frac{1}{RT}\right)\int_{V^V}^{\infty}\left[\left(\frac{\partial P}{\partial n_i}\right)_{(T,V,n_j)} - \frac{RT}{V^V}\right]dV - \ln\left[\frac{PV^V}{n_T RT}\right] \tag{4.13}$$

The liquid phase activity coefficient is determined from the Gibbs-Duhem equation:

$$\sum x_i d\ln\gamma_i = \sum x_i d\left(\frac{\overline{G}^{E}{}_{i}}{RT}\right) = \left(-\frac{\Delta H}{RT^2}\right)dT + \left(\frac{\Delta V}{RT}\right)dP \tag{4.14}$$

The activity coefficient γ_i gives the correspondence between the liquid fugacity $\hat{f}_i^L$ at condition T, P and x to some other define conditions. The other condition is referred to as the standard state and it represents the known thermodynamic condition of a component at which its activity coefficient is unity.

4.3.1 Activity coefficients

For isothermal conditions, the variable pressure activity coefficients are given by:

$$\sum x_i d\ln\gamma_i = \left(\frac{V}{RT}\right)dP \text{ (Constant } T\text{)} \tag{4.15}$$

So the use of constant pressure is an advantage, hence the equation is:

$$\sum x_i d\ln\gamma_i = 0 \text{ (Constant } T \text{ and } P\text{)} \tag{4.16}$$

The well known semi-empirical mixture models e.g. Van Laar, Margules, NRTL, UNIQUAC, etc. are particular mathematical solutions of equations (4.13) and (4.14). This equation can be applied to both symmetric and unsymmetric conventions of activity coefficients.

At low to moderate pressure the dependency of the liquid-phase activity coefficients can be neglected, thus γ_i can be considered as a function of temperature only.

At constant temperature and composition, the constant pressure activity coefficient can be calculated by the following relation:

$$\gamma^{(P^r)}{}_i = \gamma^{(P)}{}_i \exp \int_{P^r}^{P} \left(\frac{\overline{V}_i}{RT} \right) dP \tag{4.17}$$

Where $\gamma^{(P^r)}{}_i$: is the activity coefficient at an arbitrary reference pressure (P^r).

$\overline{V}_i$: Partial molar volume of pure component i.

4.3.2 Models for the excess Gibbs energy

4.3.2.1 Margules equation

Margules [1895] proposed the first Gibbs energy model. This is the oldest and the simplest activity coefficient model. The Margules equations are applicable to binary systems only and they do not deal with temperature dependence. The Margules expression is given by the equation below:

The Margules model was found very simple and limited in its ability to describe complex behaviour. It is giving a symmetric function of x_i and G^E, while most systems have an asymmetric relationship in their properties.

The Margules equations are adequate for systems with a linear dependence of G^E / RTx_1x_2 on x_1. The Margules model is suitable to mixtures with components of similar molar volumes. However it has been applied with satisfaction to various mixtures.

4.3.2.2 Van Laar equation

These equations were developed by Van Laar [1910, 1913]. The main purpose of the Van Laar model was to consider the size differences of the molecules.

The Van Laar expression works best with non-polar liquids. The Van Laar expression is flexible and simple, that is the reason why it is widely used. Some weaknesses of the Van Laar model are that: firstly it does not consider molecular interactions, and as a result, it is still poor in the characterization of highly non ideal systems, secondly, the Margules and Van Laar expression are based on an empirical foundation hence they do not give a clear understanding of

the temperature dependence and thirdly, Prausnitz et al. [1986] stated that the Van Laar model does not represent maxima or minima in coefficient activity (γ_i).

According to Malanowski and Anderko [1985] systems that give good results with the Van Laar model work badly with the two-parameter Margules model.

4.3.2.3 Wilson equation

The model proposed by Wilson [1964] is based on the local composition instead of the entire liquid composition, which is defined as the differences between a liquid solution and the total mixture composition at local composition. Contrary to the previous models the Wilson model take in account the molecular interactions.

The Wilson equations represent the temperature dependence well. It is generally good for highly non-ideal systems, however it cannot describe partial liquid miscibility or systems for which γ_i has an extremum. It is good for polar compounds. Therefore, it is superior to the Margules and Van Laar models. The Wilson model shows disadvantages can not however predict miscibility regions for a certain number of systems, and it cannot make predictions for LLE.

4.3.2.5 NRTL model

The Non-Random, Two-Liquid (NRTL) model was proposed by Renon and Prausnitz [1968] and it is used for both miscible and partially miscible systems. Equation 4.35 is the expression of this model:

$$\frac{G^E}{RT} = x_1 x_2 \left[\frac{\tau_{21} G_{21}}{x_1 + G_{21} x_2} + \frac{\tau_{12} G_{12}}{G_{12} x_1 + x_2} \right] \tag{4.18}$$

Where:

$$\tau_{ji} = \frac{g_{ji} - g_{ii}}{RT} = \frac{\Delta g_{ji}}{RT} \tag{4.19}$$

$$G_{ji} = \exp\left(-\alpha_{ji} \tau_{ji}\right) \tag{4.20}$$

α_{ij} is the non-randomness parameter

g_{ji} is the energy parameter describing the interaction between components j and i

The adjustable parameters are Δg_{12}, Δg_{21} and α_{ij}

The expressions for the activity coefficients are:

$$\ln \gamma_2 = x_2^2 \left[\tau_{21} \left(\frac{G_{21}}{x_1 + G_{21} x_2} \right)^2 + \frac{\tau_{12} G_{12}}{\left(G_{12} x_1 + x_2 \right)^2} \right] \tag{4.21}$$

$$\ln \gamma_1 = x_1^2 \left[\tau_{12} \left(\frac{G_{12}}{G_{12} x_1 + x_2} \right)^2 + \frac{\tau_{21} G_{21}}{\left(x_1 + G_{21} x_2 \right)^2} \right] \tag{4.22}$$

The use of the NRTL model is a bit demanding, because of the three adjustable parameters. According to Malanowski and Anderko [1992] the NRTL model has an advantage in the description of VLE and heats of mixing. Moreover the NRTL model gives a good description for the non-ideal mixtures Vetere, [2000]. Sandler [1997] proposed the value of 0.3 for the α_{ij}, in VLE and 0.2 in LLE

4.3.2.6 Uniquac model

The Universal Quasi-Chemical (UNIQUAC) model was developed by Abrams and Prausnitz [1975]. This model described the excess energy in two parts, a combinatorial term, which refers to molecular size and shape differences and a residual term, related to intermolecular forces. The UNIQUAC model was developed to maintain the advantages of the Wilson model, while also being able to account the partial miscibility of systems in which activity coefficients reach their extrema.

The UNIQUAC model has a wide applicability; it is suitable for nonideal mixtures. It provides explicit temperature dependence.

The UNIQUAC model has the advantages of having: applicability to multicomponent mixtures, good characterization for molecules with very large differences in molecular size, applicability to LLE.

Its main disadvantage is its complex algebraic foundation and the availability of the r and q parameters.

4.4 Equations Of State (EOS)

Equations of state (EOS) are the expressions which associate the pressure, temperature and volume of substances. There are hundreds of EOS's in the literature. The mathematical expression for an EOS is given by:

$$f(P,V,T)=0 \tag{4.23}$$

The EOS is useful in describing many properties of pure substances as well as of mixtures, such as vapour pressures, densities, critical proprieties, etc.

As presented above, on the equation 4.48, an equation of state is a function containing the pressure, volume and temperature as parameters.

4.4.1 Brief development of EOS

The concept of EOS started in 1662, with Boyle, who proposed an expression, stating that the volume of gas is inversely proportional to its pressure at a given temperature.

In 1802, Charles and Gay-Lussac calculated the effect of temperature. In 1834, Clapeyron used these results and establish the first ideal gas law:

$$PV = R(T + 267) \tag{4.24}$$

The temperature was given in ^{o}C

Further it was developed as:

$$PV = RT \tag{4.25}$$

The temperature was given in Kelvin

R is defined as the gas constant.

The ideal gas law was not able to describe real gas correctly, due to the effect of size, shape and structure, as there are some forces between the molecules which cause them to attract or to repel each other. These attractions and repulsions influence the PVT behaviour. For polar molecules

for example, these attractive and repulsive forces are very prominent with the result that the ideal gas law was inadequate for polar molecules.

4.4.2 Virial EOS

In 1927, Ursell developed the Virial EOS from statistical mechanical description of the molecular interaction in real gases. It is given by:

$$Z = \frac{PV}{RT} = 1 + \frac{B}{V} + \frac{C}{V^2} + \frac{D}{V^3} + \ldots \tag{4.26}$$

The third virial coefficient has not been extensively measured and little data is known; that is why the equation is usually truncated at the second term. As a consequence the virial equation becomes unsuitable to provide accurate enough descriptions of real gas behaviour for use in VLE calculations. The other problem that restricts the use of the virial equation is that the virial coefficients are scarcely known. Some of these coefficients have been published by Dymond and Smith [1980].

4.4.4 Cubic EOS

The cubic equations are the most useful due by the fact that they are simple, and can describe properly the vapour phase as well as the liquid phase. They are also adequate for mixtures.

Development of the cubic EOS family

The general form of cubic equation is:

$$P = \frac{RT}{V - b} - \frac{a}{g(V)} \tag{4.27}$$

$\frac{RT}{V-b}$ is represented as the repulsion pressure between molecules. b is the van der Waals volume or the excluded volume and is associated to the size of the molecules. $\frac{a}{g(V)}$ is the

attraction pressure. a is the value of the intermolecular attraction force. And the expression $g(V)$ depends on the molar volume.

Van der Waals (VdW)

Van der Waals [1873] was the first to propose a cubic EOS.

Sandler et al. [1994] stated that the van der Waals equation failed to predict vapour pressures. The van der Waals equation gives a critical compressibility factor of 0.375 for all fluids, while it should vary from 0.24 to 0.29 for hydrocarbons and the range is wider for non hydrocarbons.

Redlich-Kwong (RK)

Redlich and Kong [1949] modified the van der Waals equations and introduced the temperature dependence in the attraction term.

The RK equation gives a critical compressibility factor of 0.333, which is better compared to that of Van der Waals. The RK equation is good for approximately ideal systems as stated by Gess et al. [1991]. However the RK equation gives inaccurate values for vapour pressures prediction and liquid density.

Soave (SRK)

Soave [1972] modified the RK EOS and gave the SRK EOS. He introduced the temperature dependency into the attraction parameter:

The modification of Soave improved the prediction of vapour pressures for hydrocarbons with small number of carbons. The SRK has been widely used in the prediction of VLE at moderate and high pressures for non-polar fluids.

Raal and Mühlbauer [1998] establish that the RK and SRK EOS usually generate satisfactory vapour densities but fail to generate satisfactory liquid densities, for example the SRK EOS predicts specific liquid volumes greater than the literature values. To improve the interpretation of polar fluids Soave [1979] incorporated two empirical parameters into the expression for α function of the original SRK.

Peng and Robinson (PR)

Peng and Robinson [1976] developed the Peng-Robinson (PR) EOS. The RK and SRK EOS

were unable to accurately predict a liquid molar volume, which leads to the introduction of the PR EOS. The PR equation introduced the volume dependence:

$$P = \frac{RT}{V-b} - \frac{a(T,\omega)}{V(V+b)+b(V-b)} \tag{4.28}$$

Where:

$$a(T,\omega) = a_C \alpha(T,\omega) \tag{4.29}$$

$$a_c = \frac{0.42748 R^2 T_c^{2.5}}{P_c} \tag{4.31}$$

$$b = \frac{0.077796 R T_c}{P_c} \tag{4.30}$$

$$\alpha(T,\omega) = [1 + k(1 - T_r^{0.5})]^2 \tag{4.31}$$

$$k = (0.37464 + 1.54226\omega - 0.26992\omega^2) \tag{4.32}$$

The modifications of the PR improved the critical compressibility factor, which became 0.307. The improvement was seen also in the prediction of vapour pressures for hydrocarbons from C_6 to C_{10}. The SRK and the PR give good phase equilibrium predictions for hydrocarbon systems. They are easy to operate as they need few input data. However, they are inaccurate in liquid densities predictions and fail in phase equilibrium prediction for long chain molecules, and they show inaccurate vapour-pressure values in the critical region.

Schmidt and Wenzel [1980] introduced some modifications to the PR equation, by using the acentric factor directly as a third parameter. In the meantime Harmens and Knapp [1980] proposed the introduction of more parameters in the attractive parameter. These improvements enable the equation to predict the liquid molar volume and saturation pressure well.

Peng-Robinson-Stryjek-Vera (PRSV)

Stryjek and Vera [1986] modified the PR EOS in order to facilitate the use of cubic EOS at reduced temperatures and for better representation of some properties of polar and associating

compounds. Their EOS remains the same as the PR EOS, but there an adjustable parameter is introduced.

Alpha function

Some components (polar component) do not satisfy the conditions for the general functions that define α parameters. To compensate to this, Different expressions of α functions have been proposed, e.g. Redlich and kwong [1949], Soave [1972], Peng and Robinson [1976], Mathias and Copeman [1983], Stryjek and Vera [1986] to name a few. Except the Mathias and Copeman all these expressions have been given previously.

Mathias and Copeman [1983] proposed an α function with adjustable parameters. Below is given an expression of the Mathias Copeman with three adjustable parameters:

$$\alpha(T) = \left[1 + c_1\left(1 - \sqrt{\frac{T}{T_C}}\right) + c_2\left(1 - \sqrt{\frac{T}{T_C}}\right)^2 + c_3\left(1 - \sqrt{\frac{T}{T_C}}\right)^3\right]^2 \quad (4.33)$$

If $T>T_C$,

$$\alpha(T) = \left[1 + c_1\left(1 - \sqrt{\frac{T}{T_C}}\right)\right]^2 \quad (4.34)$$

4.4.5 Mixing rules

Most of the uses of the equations of state are on mixtures instead of the pure components. This requires the mixing rules to extend the application of equations of state to mixtures. Raal and Mühlbauer [1998] classified the mixing rules in five main categories:

1. Classical (CMR)
2. Density-dependent (DDMR)
3. Composition-dependent (CDMR)
4. Density-independent (DIMR)
5. Local composition (LCMR)

The incorporation of the local composition theory into some of these mixing rules, leads to these additional categories:

6. Composition-dependent local composition (CDLCMR)
7. Density-dependent local composition (DDLCMR)
8. Density-independent local composition (DILCMR)
9. Density and composition dependent (DCDMR)

4.4.5.1 Classical mixing rules

The classical mixing rules were developed for the van der Waals EOS. Soave made some modifications to the classical mixing rules for use with the SRK EOS.

Shibata and Sandler [1989] have found some limitations with the use of the CMR:

- The CMR fails in the prediction of liquid densities for pure fluids or mixtures with an error of 5 %. Xu and Sandler [1987a, 1987b] suggested a solution to overcome this challenge; the method is explained in their works.
- The CMR does not give a good agreement between correlated and experimental data for mixtures comprising molecules with large difference in size and/or in chemical nature.

4.4.5.2 Local composition mixing rules

For the first time the Local Composition Mixing Rule (LCMR) was introduced by Huron and Vidal [1979], and was developed further relating to the excess Gibbs free energy (G^E) to the pure component (ϕ_i) and mixture $(\hat{\phi}_i)$ fugacity coefficient.

In 1986, Danner and Gupte [1986] modified the Huron and Vidal expression and proposed a new equation, which link the a_m and b_m parameters of the EOS to the G^E at infinite pressure:

The Danner and Gupte equation has the ability to link the fugacity coefficient to the activity coefficient model via the Gibbs excess model. Tsonopoulos and Heidman [1986], stated that the

computation time is related to the cube of the number of constituents of the mixture as opposed to the square for the classical mixing rules, which is a disadvantage for the use of this mixing rule. Wong and Sandler [1992] showed another disadvantage with the use of the Huron-Vidal mixing rule, as in the low-density, the second mixture virial coefficient is not a quadratic function of composition.

Michelson, Dahl and al [1991] modified the Huron and Vidal equation to adapt it for use with the UNIFAC model. This enables the prediction of VLE data from low to high pressures.

The modified Huron-Vidal mixing rule gives good predictions of the G^E at high densities, but still not provides, in the low densities, the second mixture virial coefficient in a quadratic function of composition. Raal and Mühlbauer [1998] pointed out that the predictions of the modified Huron-Vidal mixing rule deviates significantly as the temperature and pressure range becomes very large.

4.4.5.3 Density dependent mixing rules

Mollerup [1992] proposed the introduction of density dependence into the mixing rule. This development may have helped to the problem of nonquadratic composition dependence of the second virial coefficient in the low density limit. However, Wong and Sandler [1992] stated that this development does not conserve the cubic nature of EOS when applied to mixtures.

4.4.5.4 Composition dependent mixing rules

Panagiotopoulos and Reid [1986] incorporated the influence of composition into the mixing rule. This mixing rule has the advantage of presenting a simple mathematical expression. However Wong and Sandler [1992] stated that the above mixing rule showed with some other mixing rules the problem of not having the second virial coefficient as a quadratic function of composition.

4.4.5.5 Density independent mixing rules

Wong and Sandler [1992] established the DIMR and its formulation; this mixing rule presents an advantage, in preserving the cubic nature of a cubic EOS. Instead of using the excess Gibbs free energy, the choice was made on the Helmholtz free energy.

$$b_m = \frac{\sum_i \sum_j x_i x_j \left(b - \frac{a}{RT} \right)_{ij}}{1 - \frac{A_\infty^E}{CRT} - \sum_i x_i \frac{a_i}{b_i RT}} \tag{4.35}$$

$$a_m = b_m \left[\sum_i x_i \frac{a_i}{b_i} + \frac{A_\infty^E}{c} \right] \tag{4.36}$$

Where:

$$\left(b - \frac{a}{RT} \right)_{ij} = \frac{\left(b_i - \frac{a_i}{RT} \right) + \left(b_j - \frac{a_j}{RT} \right)}{2} (1 - k_{ij}) \tag{4.37}$$

C is a constant related to the equation of state.

A_∞^E represents the Helmholtz free energy

k_{ij} represents the binary interaction parameter

The Wong-Sandler mixing rule also presents the advantage of giving good predictions in both low and high density regions.

4.5 Thermodynamic consistency testing

Data produced experimentally cannot be assumed to be absolutely accurate. In fact, Vapour Liquid measurement, especially at high pressure can be complex and source of many errors. Therefore for such judgment, the experimental data must satisfy a certain fundamental thermodynamic relationship; this process is called the thermodynamic consistency test. Liebermann [1972] stated that consistency tests verify global consistency of the experimental,

and sometimes they also assess the influence of the partial molar property of one constituent of a binary mixture from that of the other.

4.5.1 Gibb's Duhem equation

A more useful thermodynamic relationship for thermodynamic consistency testing is the Gibb's Duhem equation, which was developed in various ways.

Raal and Mühlbauer [1998] enumerated some problems encountered in extrapolating the low-pressure thermodynamic consistency tests to high-pressure. Firstly, the more volatile component is usually supercritical, which demands particular observation of the standard-state definitions. Secondly, vapour-phase nonidealities must be considered with an appropriate equation of state. Finally, the term related to liquid molar volume or excess molar volume must be evaluated.

A particular test, derived from the Gibb's Duhem equation, is the Chueh et al. [1965] Area Test; the equation below describes this test.

$$\frac{V^L}{RT} dP = \sum x_i d \ln \frac{\hat{f}_i}{x_i} \tag{4.38}$$

Further development will lead to the following equation:

$$\int_0^{x_2} \ln\left(\frac{k_2}{k_1}\right) dx_2 + \int_0^{x_2} \ln\left(\frac{\hat{\phi}_2}{\hat{\phi}_1}\right) dx_2 + \frac{1}{RT} \int_{P_1^{sat}}^{P} V^L dP = RHS \tag{4.39}$$

Where:

$$RHS = \left[\ln k_1 + \ln\left(\frac{\hat{\phi}_1 P}{\hat{\phi}_1 P_1^{sat}}\right) + x_2 \left(\ln \frac{\hat{\phi}_2}{\hat{\phi}_1} + \ln \frac{k_2}{k_1} \right) \right]_{x_2 = x_2} \tag{4.40}$$

The thermodynamic consistency test is a necessary condition but not a sufficient condition.

4.5.2 Van Ness-Byer-Gibbs test

Van Ness et al. [1973] proposed a simple and efficient thermodynamic consistency test which consisted of plotting the residual vapour mole fraction (calculated vapour mole fraction minus experimental vapour mole fraction) against the experimental liquid mole fraction. If there is a good scatter of the points along the zero x-axis the experimental data satisfies the thermodynamic consistency test. Jackson [1995] applied successfully this method and stated that it's the most definitive thermodynamic consistency test currently available; by the way, He recommended that the average magnitude of the y-residual must be less than 0.010.

4.6 Conclusion

Mühlbauer and Raal [1995] and Ramjugernath and Raal [1999] stated many difficulties with the application of the combined method to HPVLE, and it was found that the direct method correlate well the HPVLE. The correlation becomes even better with the application of the modern direct method as stated by Mühlbauer and Raal [1998]. The modern direct method incorporates into the vapour and liquid phase fugacity coefficients, the activity coefficients by the use of mixing rules, thus combining the EOS and the activity coefficient model.

According to previous works on refrigerant systems, such as those of Coquelet et al. [2003], Madani et al. [2008a], Madani et al. [2008b]; the best model for these systems at high pressure is the combination of the Peng-Robinson EOS incorporating the Mathias Copeman alpha function, using the Wong Sandler mixing rule with the NRTL activity coefficient.

CHAPTER 5: EXPERIMENTAL EQUIPMENT

The apparatus used in this study incorporated the static analytic measurement method, similar to that described by Naidoo [2004] and Naidoo et al. [2008]. It is presented in Figure 5-1. The main sections of the experimental apparatus are:

- The equilibrium cell
- An agitation mechanism for the equilibrium cell contents
- Liquid and vapour sampling methods
- The air bath
- Devices for temperature, pressure and composition measurement.

As stated in chapter I, one of the aims of this work was the modification of the apparatus. These modifications were based mainly on the sampling technique. Naidoo [2004], suggested that the sampling technique be modified. It was observed that the sampling analysis of both vapour and liquid phases took longer than desired. The Rapid Online Sampler Injector (ROLSI^{TM}) was introduced in the apparatus to replace the previous sampling method, which comprised a couple of valves and the jet-mixers. More details about the modifications are described in this chapter.

5.1 Equilibrium Cell

The equilibrium cell was made from a solid 316 stainless billet of diameter 60 mm and height 100mm. The 316 stainless steel was used because of its magnetic properties and inertness to organic materials. To eliminate any differential expansion or corrosion problems that may occur due to the use of different materials of construction, only 316 stainless steel was used throughout the whole apparatus, unless when other material was required to fulfil a specific function which required a specific materials property. A cylindrical cavity of 30 mm diameter and length of 85 mm was drilled in the billet, and provided an internal volume of approximately 60 cm^3.

Two viewing windows were placed on the sides of the equilibrium cell; they allowed the visual observation of the cell contents. In this way, one could be able to control the adjustment of the capillary of the ROLSI^{TM} into the liquid or the vapour phase; it also helped to control the

amount of component introduced in the cell and the liquid level in the equilibrium cell. The windows were manufactured from synthetic sapphire, which could withstand a pressure up to 20 MPa. These windows were 15 mm thick and 33 mm in diameter. The viton "O" rings ensured sealing between the sapphire windows housing and the equilibrium cell body.

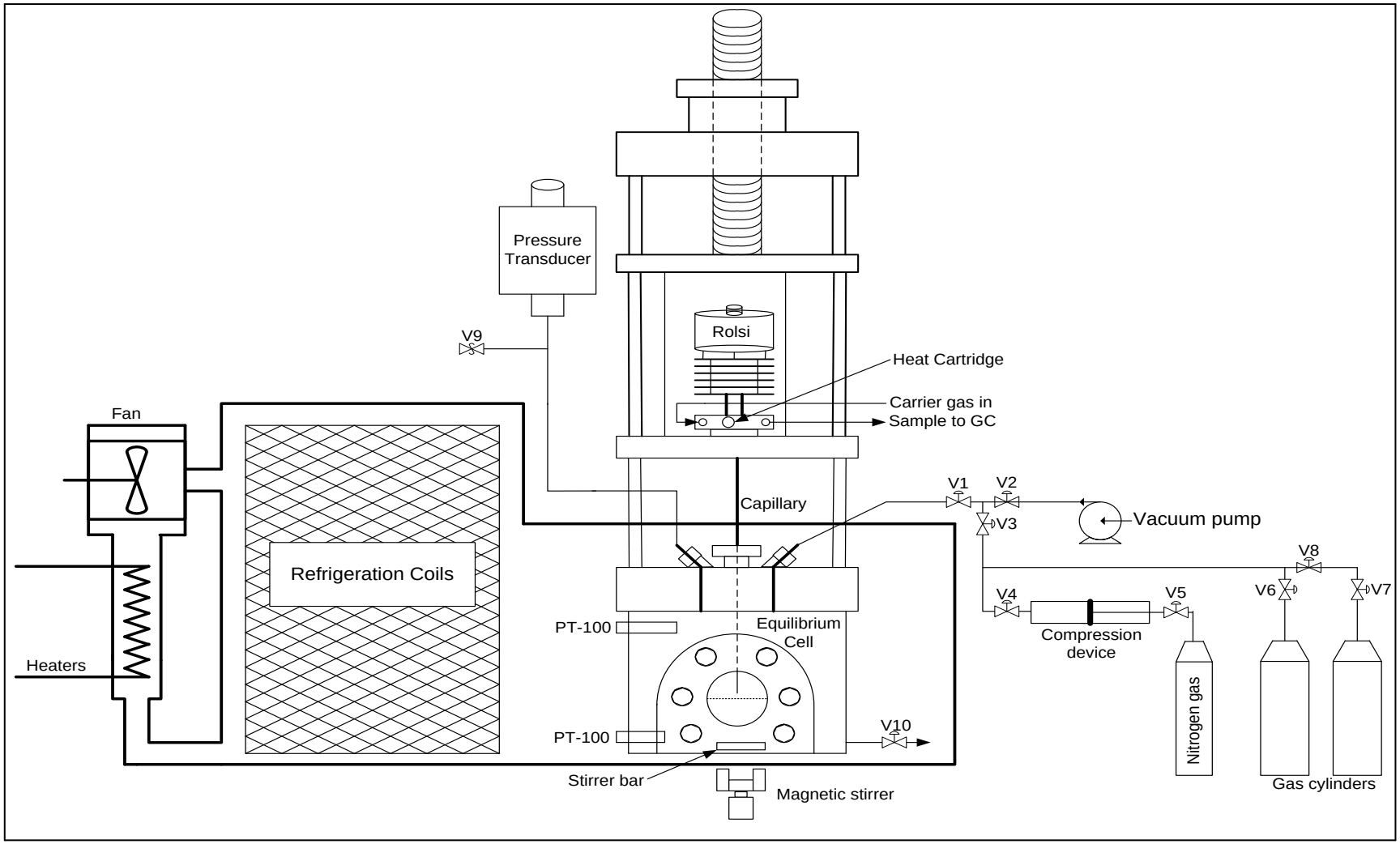

Figure 5-1: Schematic diagram of the static analytic apparatus. v_i: valve

The windows were surrounded by gasket material and tightly fixed and sealed into stainless-steel housing by means of viton „O' rings. Sealing between the gasket material and the rest of the apparatus was also ensured by the viton „O' rings. Five 8 mild steel bolts secured each sapphire window to the equilibrium cell.

Three holes of 3 mm diameter were drilled in the equilibrium cell chamber, the first hole was used for filling and evacuation of the cell contents; it was positioned on the top of the cell. The second hole was positioned at the bottom of the cell to drain any remaining liquid in the cell and the third linked to the pressure transducer; it was also located at the top of the cell. The diameters of these lines were made as small as possible to minimize the dead-volume in the equilibrium cell.

The drain valve and the fill and evacuate valve for the cell were Whitey valves while the rest of the valves used on the apparatus were Swagelok. The fill and evacuate valve was tri-directional whereas the drain valve was bi-directional and both were able to handle a temperature and pressure combination of 423 K and 17 MPa respectively. The tri-directional valve was connected to the gas bottle (or the compression device), and to the equilibrium cell, while the third end linked to the fume cupboard.

The capillary of the sampling apparatus (ROLSI^{TM}) was inserted into the equilibrium cell from the top and was adjusted with a fitting in the centre. The sampling apparatus was connected to a screw for guidance. Thus the operator could adjust it such that the capillary could sample either from the vapour phase (top) or the liquid phase (bottom).

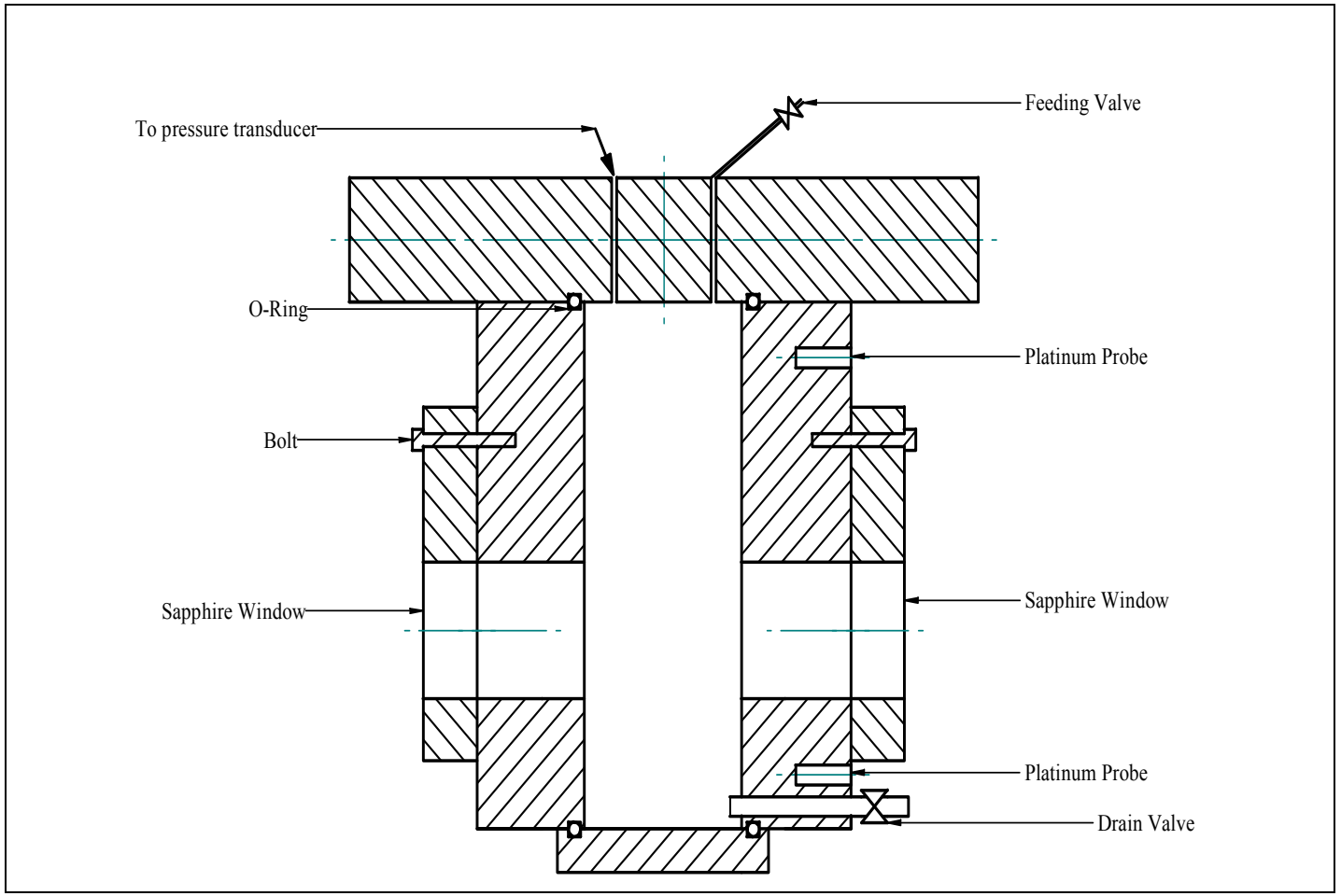

Figure 5-2: Equilibrium cell

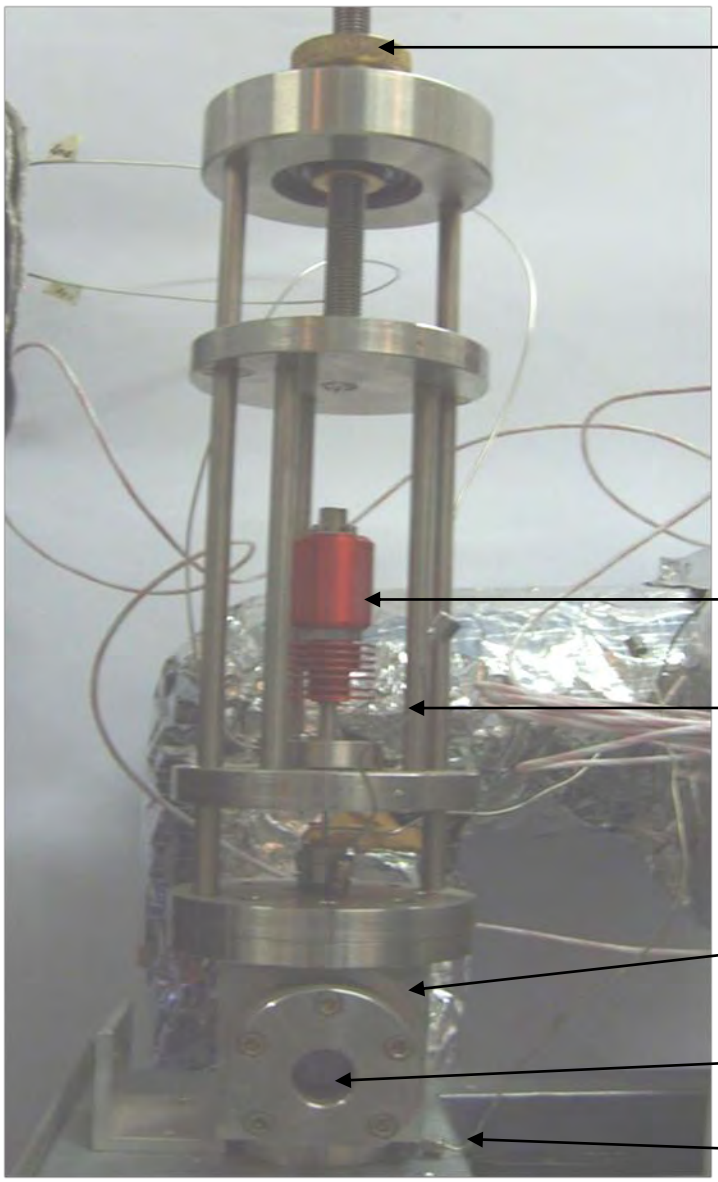

Photograph 5-1: The equilibrium cell of the static VLE equipment connected to the ROLSI™.

5.2 Agitation of cell contents

Unlike the dynamic method where the vapour and liquid phase are in permanent contact, the static method requires significant time to reach equilibrium. The phases are motionless and do not mix with each other. Agitation was therefore introduced to accelerate the process. The cell

contents are agitated by the means of an impeller. The impeller has embedded rare earth magnets. The role of the impeller was to achieve good mixing of the liquid phase and hence decrease the equilibration period.

The agitation allowed entrainment of the vapour into the liquid phase; as a consequence increasing of the rate of mass transfer. The impeller was manufactured from type 316 stainless steel and was mounted on a stainless steel pin. The rotation was produced by direct magnetic coupling to a horse-shoe magnet mounted on a Maxon motor in a well beneath the equilibrium cell body, which was also acting as a support for the cell body. The Maxon motor ran at a maximum voltage of 12 V DC, the current was supplied by the means of a 500 mA adaptor.

5.3 Liquid and vapour sampling method

This section outlines the main modifications undertaking in this project. Previously, complex sampling techniques were used. The sample was taken by the use of a six or eight port two position GC sampling valve. In the sampling position of the valve, the fluid filled the sampling loop, and in the flushing position the fluid was transported to the GC by the carrier gas. To overcome the problems of the tendency of the more volatile component to flash preferentially, (encountered in the static method), a jet mixer was added in the process. This sampling technique was difficult, time-consuming and a source of errors. One could expect to spend not less than four hours for analysis of a single equilibrated vapour or liquid data point.

This led to the introduction of a new method, which seemed more accurate and easier to operate. The new method of sampling incorporated the use of the Rapid Online Sampling Injector (ROLSI^{TM}), this technique was described by Guilbot et al. [1998].

Sampling was controlled entirely electronically. Moreover the ROLSI^{TM} had the ability to work at various temperatures. The mass of withdrawn samples depends on the pressure of the equilibrium cell content but also on the opening time of the ROLSI^{TM}, which was between 10 milliseconds and 100 seconds. The ROLSI^{TM} was specially developed for sampling at high pressures and the analysis of samples by gas chromatograph. It was directly connected to the equilibrium cell, hence to allow the in situ removal of repeated representative samples from the medium to be analyzed without any contamination of it. It had an incorporated heating system and, it allowed the instant vaporization of the liquid sample. Its maintenance proved to be easy and inexpensive.

Main specifications of the ROLSI^{TM} are:

- No dead volume
- Practical and highly automated.
- Gives representative samples.
- The method is rapid, 30 min was sufficient to have an analysis of a pair of points.
- Variable sample volume between 0.1 mg and few mg.
- Ability to have an instant vaporization of liquid samplings
- Very large range of operating temperature: from cryogenics to 553 K (for continuous operation) and to 583.15 K (for time ranges less than 30 minutes).
- Very large range of operating pressures: from atmospheric pressure to 60 MPa.
- Body made of 316 stainless steel.
- Dimensions of the capillary : length 11 cm, external diameter 1 mm and internal diameter 0.1-0.15 mm

The ROLSI^{TM} sampler injector had a capillary with one end connected to the site which needs to be sampled and received a continual flow of helium gas from the cylinder via the gas chromatograph. The seal of the capillary (the end connected to the body of the sampler) was secured by a moving part and the other end consisted of a soft iron core pushed in the direction of the capillary by a helical spring.

The ROLSI^{TM} used in this project was a movable ROLSI^{TM}, with the advantage to take both vapour and liquid samples, by the means of its ability to move into both phases. Special fittings were required on the equilibrium cell to allow movement of the ROLSI^{TM}. A nut, from which the capillary of the ROLSI^{TM} penetrated into the cell, was mounted on the flange of the cell. Viton „O' rings were used to ensure sealing between the capillary of the ROLSI^{TM} and the nut.

Sampling was initiated by signalling the electromagnet, which attracted the moving part, moving it away from the capillary and breaking the seal between the fixed capillary and the moving point. The size of the samples taken, under the given pressure and temperature conditions, was directly proportional to the seal-break time (opening time). This time was controllable, as well as the delay between taking two samples by means of a timer coupled with the electromagnet's power supply. The ROLSI^{TM} was connected to an adjustable screw, in order to facilitate the adjustment of the capillary into the liquid or the vapour phase according to the need.

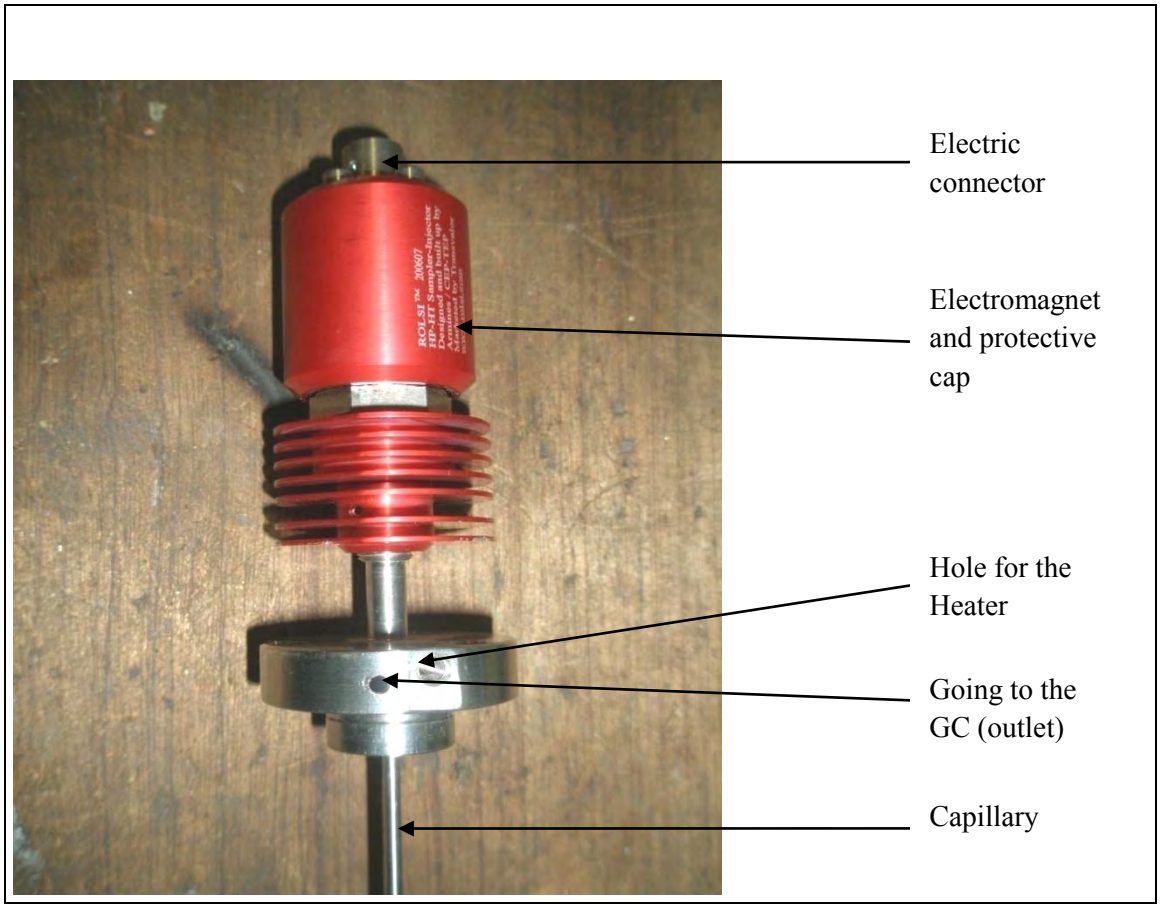

Photograph 5-2: The ROLSI^{TM}

5.4 Air bath

To create an isothermal environment, the equilibrium cell was immersed in an air bath, thus minimizing the temperature gradient inside the cell. This state was attained by the circulation of air in the bath through the heating apparatus by means of fan and the temperature of the air was controlled.

The bath was a rectangular box 0.35 m in length, 0.23 m in width and 0.29 m height. The box was manufactured using 4 mm thick mild steel plates which had been joined. To ensure total insulation, the bath lid was sealed with fibrefrax.

The dimensions of the air bath were modified in this project. The previous air bath was 1 m length, 0.75 m width and 0.5 m height. This bath was constructed to contain the cell and all the sampling devices, which comprised the lines, valves and jet-mixer. As the sampling technique was modified with all the previous devices (lines, valves, jet-mixer) being replaced by a single ROLSI^{TM} which was attached to the cell, this freed a lot of space in the bath. The bigger the

bath, the bigger the temperature gradient inside the cell therefore the bath was modified to smaller dimensions, ameliorating the temperature profile.

The fan was rotated by a single phase electrical motor of 230 V, 2.65 A, 50 Hz, 0.37 kW and 2820 rpm (as maximum speed). The fan blew in air, which circulated throughout the compartment which contained the heaters and cooling coils. This compartment was situated on the left of the air bath. The air circulated from that compartment to the bath. The heaters were not placed directly in the bath to avoid an irradiation effect on the cell, this phenomena was reported by Bradshaw [1985].

As soon as the required temperature was attained, it was controlled to maintain a stable environment in the air bath. The air bath allowed a rapid attainment of thermal equilibrium which took approximately 45 minutes, as opposed to the previous larger air bath which took on average 12 hours (overnight) to equilibrate.

5.5 Heating and cooling devices

For temperatures different from the ambient temperature (low temperature or high temperature), cooling and heating devices were used on different parts of the equipment as needed.

5.5.1 Cooling device

The refrigeration apparatus incorporated a condenser, an evaporator; a compressor and a throttling valve (refer to Figure 4-3).

The condenser and the compressor were incorporated in a single unit, manufactured by L'Unité Hermétique from France. The condenser worked at a maximum outlet pressure of 1.8 MPa. The condenser was cooled by a fan.

The construction of the evaporator was similar to the condenser. The compressor/ condenser unit was external the bath while the evaporator coils were located in a steel box which was adjacent to the air-bath.

.

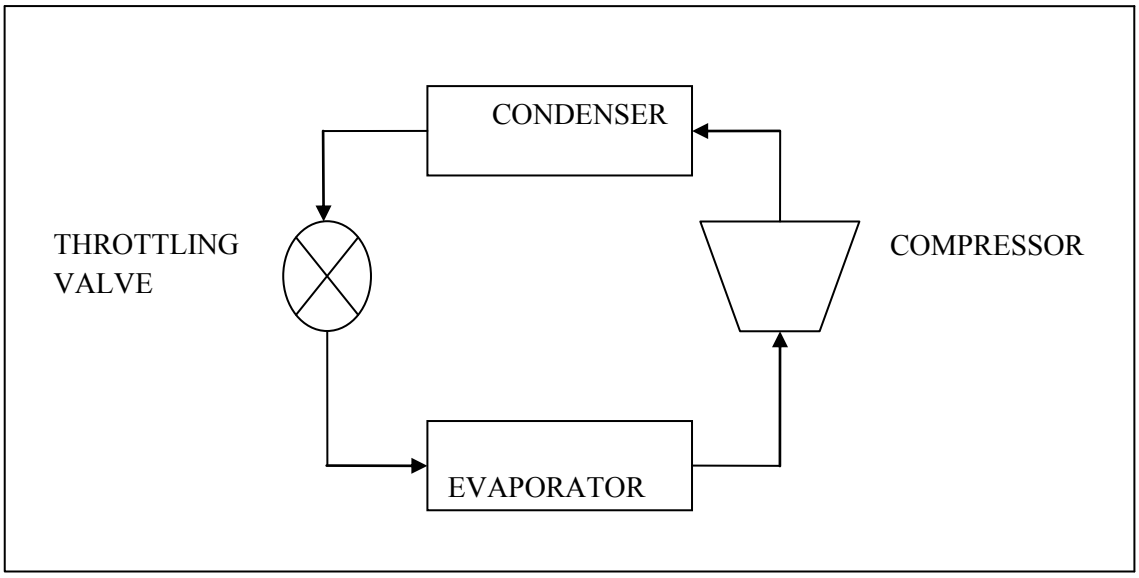

Figure 5-3: The Refrigeration Unit

5.5.2 Heating device

5.5.2.1 Heaters

For high temperatures in the air bath, two heaters of 300 W and 220 V each were used. They were activated by a temperature controller via a relay. The relay was used to switch the heaters on and off. The relay received the signal from the bottom sensor (from the cell). The load side of the relay was powered by a 220 V plug. The coil side of the relay was powered by the controller 220 V AC. The parameters of the controller were set by auto tune.

5.5.2.2 Heater Cartridges

- Two heater cartridges of 6 cm length, 3 mm diameter, 230 V and 80 W each were housed in the block which kept the pressure transducer at a fixed temperature. The pressure transducer is very sensitive to temperature despite precautions set by the manufacturer. Fluctuation of the ambient temperature influences the sensitivity of the pressure transducer, and leads to erroneous pressure measurements. For one to get an accurate and precise reading of pressure, the transducer was kept in a box which was heated and maintained at 313.15 K.

- Two heater cartridges of 6 cm length, 3 mm diameter, 20 V and 50 W each were used for the blocks which heated the 6 ports valve. To avoid condensation of the sample in the 6 ports valve, the 6 ports valve was heated and maintained at 353.15 K.

- One heater cartridge of 230 V and 100 W was used to heat the ROLSI^{TM} for instant vaporization of the liquid sample. It was an L shape heater cartridge with a 3 mm diameter.

5.5.2.3 Nichrome wires

All the lines used to carry the sample to the GC and the line connecting the pressure transducer to the equilibrium cell were kept heated using nichrome wires supplying electricity by variacs of 220 V AC input and 0 to 250 V AC output. The reason for heating the lines was to avoid condensation of the sample while it was sent to the GC for analysis.

5.6 Devices for measurement

5.6.1 Pressure

The pressure measurements were recorded on electronic displays connected to the pressure transducer. A Sensotec Model TJE transducer with a range of 0-15 MPa was used for pressure measurement. This transducer was certified as having 0.25% accuracy of the entire scale pressure of the instrument. The transducer was connected to an Agilent data acquisition unit (34970A), and this unit was connected to a computer via a RS-232 interface. Hence one was able to obtain not only the pressure value, but also, the real time reading and save different pressures and temperatures measurements throughout the experiments. The transducer was calibrated before any measurements; the stated uncertainty was of $\pm$ 4 kPa in the range of 0.1 to 6 MPa.

5.6.2 Temperature

Temperature measurements were made using platinum resistance thermometers (Pt-100). For the equilibrium cell, two Pt-100s were used. They were supplied by WIKA, with an accuracy of $\pm$ 0.15 K in the range of 73.15 K to 1073.15 K. These probes were fixed separately in the wall of the equilibrium cell body, one at the top of the cell and the other at the bottom. These locations corresponded to the vapour and liquid phase respectively. The probes were L shaped; the short part went into the wall of the cell while the long part remained outside. The short and the long part were about 0.05 and 0.15 m long respectively. Two class A Pt-100s were chosen in order to perform accurate temperature measurements in the cell and to check for thermal gradients. Both Pt-100s were connected to the same Agilent data acquisition as the pressure Sensotec readout.

The ROLSI^{TM} temperature was monitored by a small glass Pt-100 placed inside its body. The ROLSI^{TM} device provided for a hole for the temperature device. The ROLSI^{TM} was heated and maintained at 353.15 K.

Temperature measurement at different points that required a control of temperature (pressure transducer block, sampling lines, compression device, etc.) was performed by means of class B Pt-100s as high accuracy was not required.

For the control of all the temperatures quoted previously, ACS Shinko 08KF00974 temperature controllers were used. These controllers were supplied with 100-240V AC 50/60 HZ, with an output of 12V DC. They are PID controllers with the auto-tuning and adaptive tuning abilities.

5.6.3 Composition

The liquid and vapour sample compositions were determined by gas chromatography. The sample passed through the 6 port valve before entering the GC. This avoided overloading of the GC. Figure 4-4a and 4-4b show the configurations of the 6-port valve. This could be used in two positions: position 1, the sampling position, and position 2, the flushing position.

In the sampling position, a sample charged the loop while the helium gas entered the valve by port 2 and exited the valve through port 1 to the GC hence ensuring the cleaning of the loop.

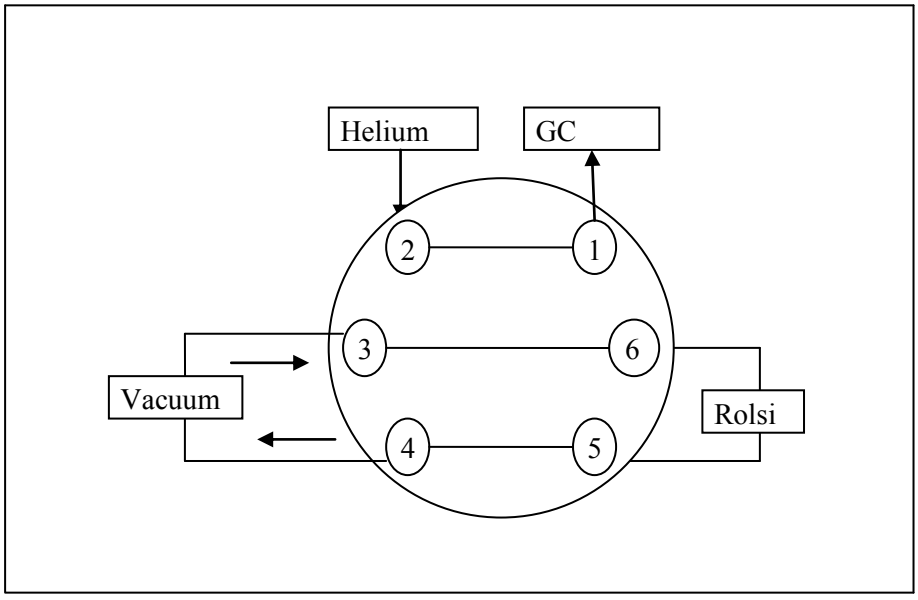

Figure 5.4a: 6 port-valve in the sampling position

In flushing position, helium gas flushed the sample out of the sample loop to the GC, while the remaining sample was vented by the use of the vacuum pump.

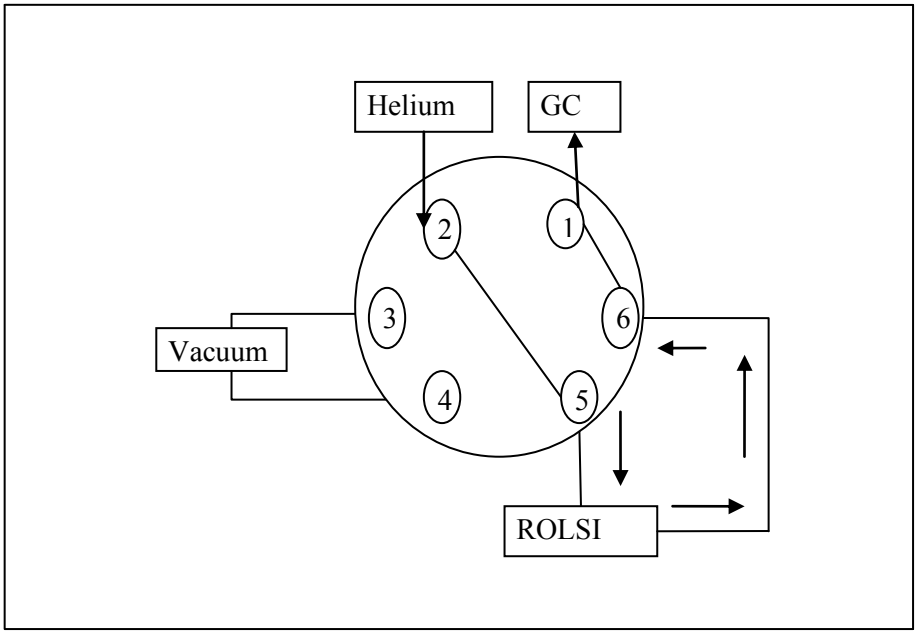

Figure 5.4b: 6 port-valve in the flushing position.

The 6-port valve was manufactured by VALCO and it is specified for high pressures (17.5 MPa) and high temperatures (473.15 K).

All composition analysis were performed using a Shimadzu, Model 2010 GC equipped with a Thermal Conductivity Detector. The components were separated using a Porapak Q column which had a length of 2 m, inner diameter 2.20 mm, 80/100 mesh and film thickness 100 μm. All the settings for the injector, the column as well as the detector are provided in Chapter 6.

5.7 Auxiliary device

5.7.1 Compression device

For any gas with a low vapour pressure at ambient temperature, a compression device was used to obtain pressures higher than the bottle pressure. The compression device was designed by Ramjugernath [2000] and consisted of two compartments. One of the compartments was filled with the gas that need to be pressurized and was constructed with type 316 stainless-steel billet.

The other compartment received nitrogen from a high pressure cylinder (the nitrogen pressure was approximately 25 MPa).

The two compartments were joined by the use of 12 high tensile, 8 mm steel cap head screws, aligned by a spigot. A piston with double head converted the pressure of the nitrogen compartment to the gas in the other compartment. Two sets of Viton "O" rings were used to ensure a firm seal between the piston and the compartments.

The compartment which received the low vapour pressure gas was heated by the means of three heater cartridges of 150W and 250V. The three heater cartridges were placed at the same distance all along the circumference in the wall of the compartment. A variac voltage alimented the heater cartridges. A Pt-100 was placed in the wall of the compartment to measure the temperature. The heating procedure facilitated the attainment of relatively high pressures.

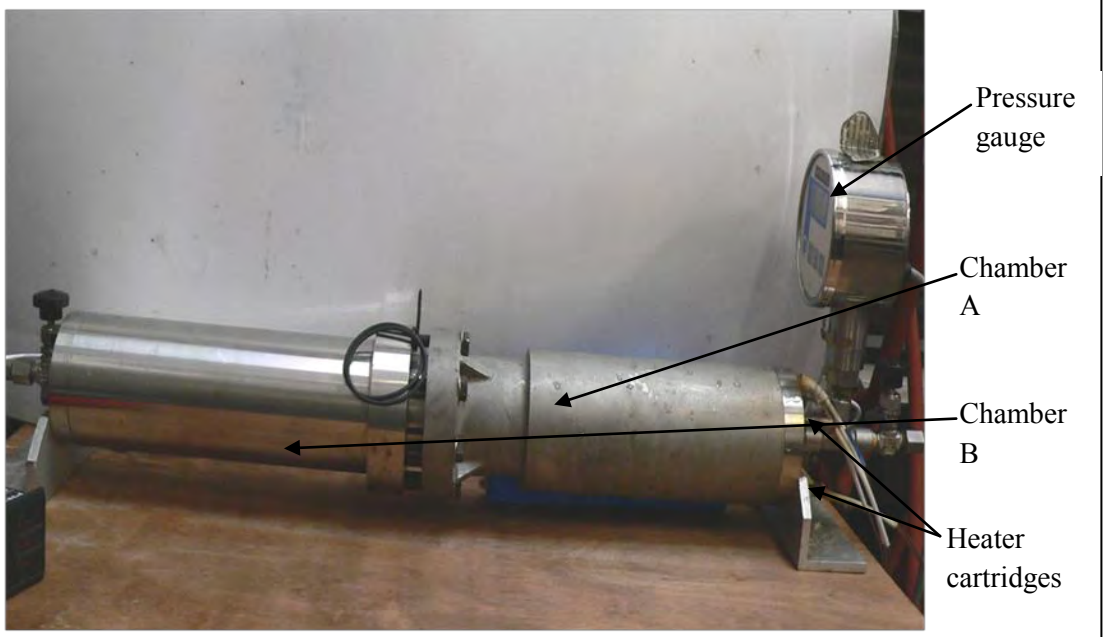

Photograph 5-3: The Compression device. Compartment A: received gas to be compressed; Compartment B: received nitrogen at high pressure.

CHAPTER 6: EXPERIMENTAL PROCEDURE

The accuracy of HPVLE data is directly related to the effectiveness of the experimental procedure hence one should carefully design and enact the experimental procedure and avoid all sources of error during the experimental process.

Things that generally affect results in HPVLE are the temperature, pressure and composition calibration. This is crucial for accurate results. Methods and some recommendations during these calibrations are presented in this chapter.

The method used by Ramjugernath [2000] served as basis for the current experimental procedure; however some modifications were added as required to deal with to difficulties encountered along this project.

6.1 Preparation of experimental equipment

6.1.1 Preparation of the equilibrium cell

The measurement of pressure is an important task in VLE studies so it is mandatory to ensure that there are no leaks in the equilibrium cell, especially when it comes to high pressure measurement. One should also avoid leaks in the lines that convey the sample to the GC.

Before any experimentation, leak testing was undertaken and as follows: the equilibrium cell and all the auxiliaries lines are pressurized up to a certain value, for instance 14 MPa. After twenty four hours, if the drop of pressure can be attributed to only the drop of the ambient temperature, then the apparatus is ready for experimentation. If not, this means that the vessel or lines cannot hold the pressure and they are leaking. With the use of Snoop®, leaks are located and fixed. Generally leaks were found on the threaded fittings of screws etc and lock tight or thread tape was used to improve sealing.

To avoid any contamination of the investigated system, the cell was cleaned before every run. The cell and all the auxiliary lines were heated to 328.15 K (this value depends upon the type of component used) and placed under vacuum for a minimum of 10 hours. After this process all the valves were kept closed, hence the cell remained under vacuum until the component was filled.

The sampling lines were cleaned by flushing with the carrier gas.

6.1.2 GC calibration

For the determination of both vapour and liquid compositions, the GC2010 Gas Chromatograph was used. In order to analyse for compositions the detector had to be calibrated. There are two methods of calibrating a TCD GC; the direct injection method and the internal standardization method. For this work, the direct injection calibration method was chosen. A brief description of the method is given below.

By injecting, with a syringe, different known volumes of a pure component, one is able to generate a curve of GC peak area (A) versus number of moles (n).

$$n_i = C_{1i}A_i^2 + C_{2i}A_i + C_{3i} \tag{6.1}$$

C_{1i} , C_{2i} , C_{3i} are the response factors of component i .

Since only gas components were used for this project, a presentation of a GC calibration method for gases is presented below.

6.1.2.1 Gas component calibration

The gas sample was withdrawn from the cylinder via a tube connection with a septum fixed at its end. Thus the gas syringe could easily penetrate the tube through the septum. Known volumes of gas samples were withdrawn from the bottle and injected into the GC with the appropriate syringe (gas syringe). Withdrawal of gas and injecting into the GC had to be done quickly as the longer one takes the more gas is lost from the syringe, which introduces errors into the calculations. The injections were repeated for verification. Attention was required while using the syringe to reproduce the exact volumes. The equation of peak area versus the number of moles was generated. All the calibrations done in this project were performed with an absolute deviation of the peak area from the calibration equation as a function of number of moles not exceeding 3%.

The number of mole of component was calculated using the ideal gas law:

$$n = \frac{PV}{RT} \tag{6.2}$$

V is the volume of the sample injected in m^3

T is the temperature of the injected gas (ambient temperature in K)

R is the Universal gas constant

P is the Pressure of the injected gas (atmospheric pressure in Pa)

6.1.2.2 Precautions taken during calibration

As the composition analysis required a high degree of accuracy, the GC calibration procedure demanded as well the highest level of accuracy, much attention and precision are required from the person who is doing it.

One had to make sure that the same volume of gas was taken in the syringe to obtain reproducibility of peaks. The syringes used had to be of a good quality which means the piston plunger seal was tight in the body of the syringe and the needle was not blocked.

Before injecting any sample, the syringe was flushed with the component used approximately two or three times to avoid contamination.

After each 100 injections, the GC injector septum had to be replaced to avoid entrainment of air in the GC column.

6.1.3 Temperature calibration

The platinum probes used to measure the temperature in the equilibrium cell were initially calibrated. Both Pt-100 were calibrated against the standard CTH 6500 probe manufactured by WIKA. This standard had a stated accuracy of $\pm$ 0.05 K in the range of 73.15 to 473.15 K. The CTB 100 Micro calibration bath was used to set the temperature. The operation was repeated three times, necessary to ensure accuracy. The uncertainty of the calibration for both probes was $\pm$ 0.02 K.

6.1.4 Pressure calibration

The pressure transducer used for pressure measurement in this project was calibrated against a standard CPH 6000 process calibrator, manufactured by WIKA. The standard transducer had a stated accuracy of 0.025% in the range of 0 to 25 MPa. A manual test pump was used to generate pressure. Anatmospheric pressure reading was required as the apparatus read the relative pressure. A barometer was used for the atmospheric pressure reading. The test was done three times for a good accuracy. The calibration was done with an uncertainty of $\pm$ 4 KPa in the range of 0.1 to 6 MPa, which 4 to 0.07% increasing the pressure.

6.2 Start-up procedure

As the cell was cleaned under vacuum to avoid contamination, all the valves were closed to maintain the vacuum within all the lines and the cell.

The equilibrium cell was charged initially with the least volatile component and thereafter successive amounts of the more volatile component were added.

The first component was filled until one obtained a liquid phase of it in the cell. The second component was filled from its cylinder according to the required pressure. When the required pressure was higher than the pressure in the gas cylinder, the compression device was used to obtain the desired pressure. While the system temperature was set on the temperature controller and the air-bath was heated or cooled according to the set temperature, the stirrer was fixed at the maximum speed to provide vigorous stirring for almost 30 min, then the speed was decreased to the normal setting (moderate rate).

The system was left to equilibrate. When the pressure stayed stable for about 30 min, this was a sign of equilibrium and the system was ready for sampling.

6.2.1 Positioning of the liquid-level

While adjusting the pressure of the cell, the liquid-level can rise considerably and can also fill the cell entirely. Consequently droplets of liquid phase can be found in the vapour sampling line; one cannot then distinguish the liquid phase from the vapour phase during the sampling procedure.

However, if the liquid-level is too low the quantity of the liquid may be insufficient for sampling and this leads to an incorrect composition analysis.

It was necessary to keep the liquid-level at a suitable level which is half way up the sapphire window. When the liquid level goes too high, the operator can reduce it by opening the drain valve of the equilibrium cell and adjust the liquid level at the appropriate position.

6.3 Sampling procedure

The sampling process was by means of the ROLSI^{TM}. The ROLSI^{TM} was connected to a timer control, and two times were set. The first time set represented the time between samples Since many samples were required to be taken, a certain period of time was necessary to separate different samples in order to avoid overlapping of the corresponding peaks area on the GC. The second time setting, called the opening time, was for the removal of the sample. This time was set according to the pressure inside the cell and range of the corresponding GC calibration. This means the response of the TCD should be comprised in the range of the calibration.

As mentioned before, both vapour and liquid sample were withdrawn using the ROLSI^{TM}. The capillary was adjusted in the vapour or liquid phase when the vapour or liquid phase respectively was to be analysed.

An adjustable screw sets the position of the ROLSI^{TM} either in the vapour or liquid phase. Many samples were removed from the cell until having a good repeatability (less than 1%). The stirrer was set to its lowest speed while samples were withdrawn to avoid unexpected flushing or splashing of liquid into the vapour phase or entrainment of vapour bubbles in the liquid phase.

CHAPTER 7: RESULTS AND DISCUSSIONS

In this chapter different aspects of the research will be presented, such the accuracy of the measured variables, the GC calibrations, pure experimental data, and experimental VLE data with comparisons to values from the literature, experimental VLE data for the unknown system with the thermodynamic modelling.

7.1. Purity of materials

7.1.1 Propane

The propane was supplied by Afrox and the purity was stated to be 99.92%. The main impurities were air, ethane and water. Propane was used in the experimental measurements for the test system.

7.1.2 Hexafluoroethane (R116)

The R116 was supplied by Air Products with a stated purity of 99.95%. The main impurities were ethane, n-butane, isobutane, ethylene, oxygen and argon.

7.1.3 Hexafluoropropylene oxide (HFPO)

The HFPO was supplied by NECSA with a stated purity of 99.99%. The main impurities were Hexafluoropropene (HFP) and Hexafluoroacetene (HFA).

7.1.4 Ethane

The ethane was supplied by Air Products with a stated purity of 99.00%. The main impurities were air, methane and water.

7.1.5 Helium

The helium was supplied by Afrox with a stated purity of 99.99%. Helium was used as a carrier gas for the gas chromatograph.

7.2 GC calibration

Fixed amounts of pure gases were injected into the GC at different volumes from 0.05 ml to

1 ml. By knowing the injected volume, the ambient temperature and pressure, one determines the number of moles of standard injected. The equation related the peak areas and the number of moles was determined, and it was a polynomial equation of second order (equation 6.1)

The details of calculations about the calibration equations and the relative deviation are given in Appendix B. The coefficients C_1, C_2 and C_3 for the components used in this study are provided in Table 6-1 and the plots of the relative deviation versus the number of moles are shown in Figures 7-1 to 7-4.

Table 7-1: Coefficients obtained for the GC calibration equations

Component i	C_{1i}	C_{2i}	C_{3i}
Propane	$-1.0828*10^{-28}$	$-2.7694*10^{-12}$	$-1.6710*10^{-07}$
R116	$-5.4100*10^{-22}$	$2.7694*10^{-12}$	$-1.6710*10^{-07}$
Ethane	$-9.3221*10^{-21}$	$1.9654*10^{-12}$	$2.2966*10^{-07}$
HFPO	$-6.6425*10^{-21}$	$1.1890*10^{-12}$	$7.7836*10^{-07}$

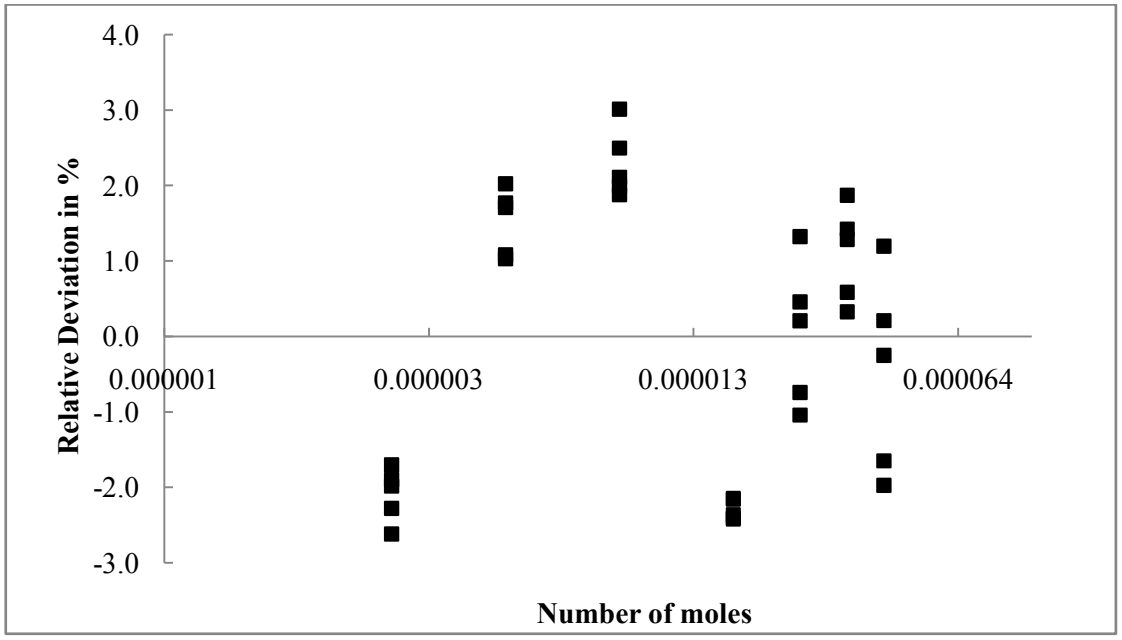

Figure 7-1: Relative deviation of propane vs. the number of moles

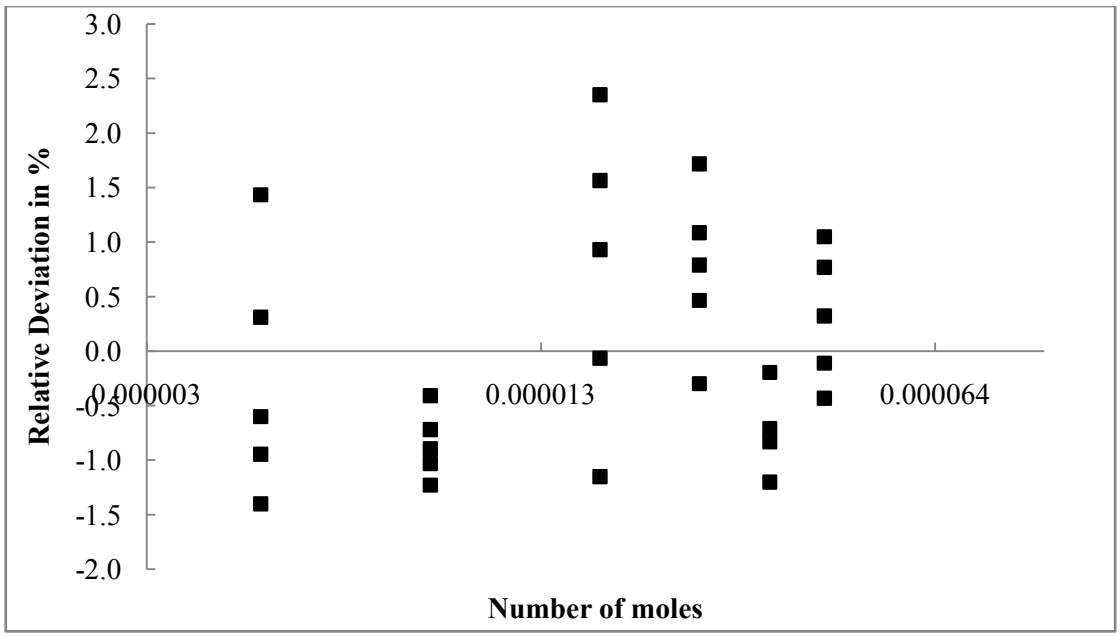

Fig 7-2: Relative deviation for R116 vs. the number of moles

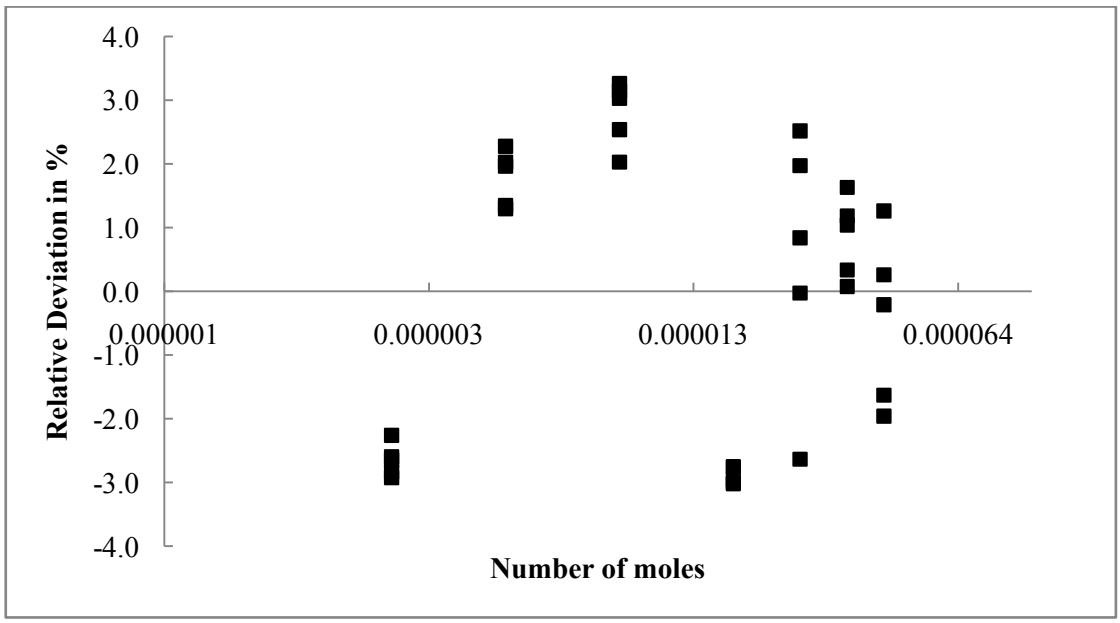

Fig 7-3: Relative deviation for ethane vs. the number of moles.

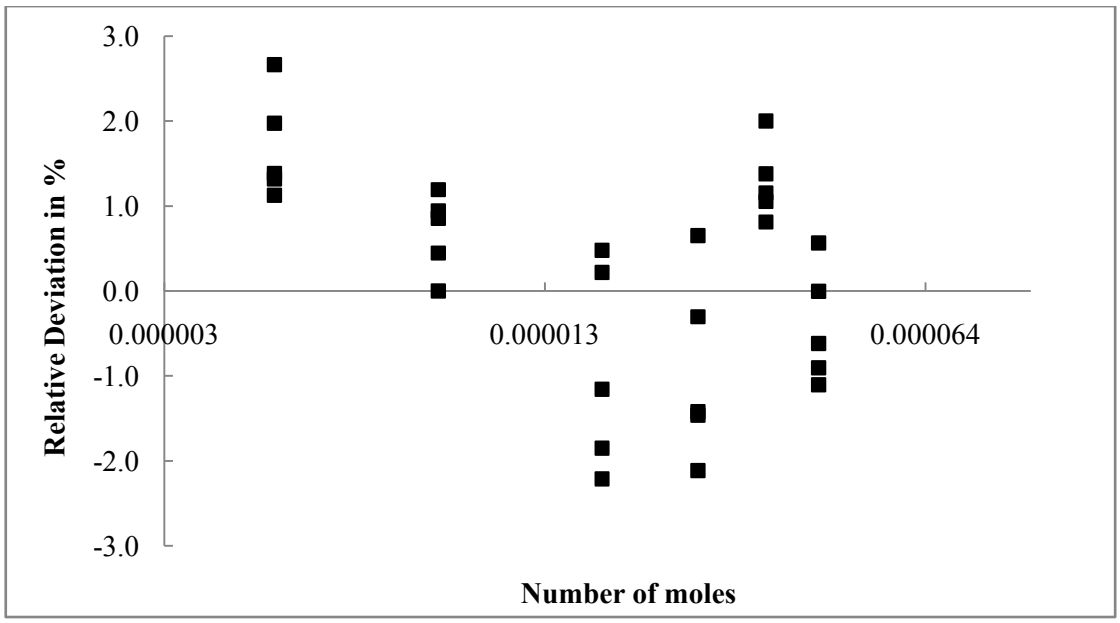

Fig 7-4: Relative deviation for the HFPO vs. the number of moles

7.3 GC operating conditions for VLE measurements

Operating conditions of the GC differ for each system investigated. The operating conditions of both the R116 + Propane and Ethane + HFPO systems are presented in Table 7-2**.**

Table 7-2: GC operating conditions

OPERATING CONDITION	R116 + PROPANE	ETHANE + HFPO
Injector temperature	160^{o}C	110^{o}C
Flow control mode	Pressure	Pressure
Injection mode	Split	Split
Pressure	150 kPa	150 kPa
Total flow	220 ml/min	220 ml/min
Column flow	10 ml/min	10 ml/min
Purge flow	0.5 ml/min	0.5 ml/min
Linear velocity	100 cm/sec	100 cm/sec
Split ratio	0.0	0.0
Column temperature	130^{o}C	90^{o}C

OPERATING CONDITION	R116 + PROPANE	ETHANE + HFPO
Equilibration time	1 min	1 min
TCD injector temperature	170°C	150°C
Stop time	50 min	50 min
Current	90 mA	90 mA

Table 7-3: Column specifications

Column	Poropak Q
Serial number	1643
Column max temperature	250°C
Length	2 m
Inner diameter	2.20 mm
Film thickness	100 µm
Mesh	80/100

7.4 Experimental results

7.4.1 Vapour pressure measurements

Vapour-pressure measurements were performed for two different pure components, propane and ethane. The experimental data were compared to the literature. The Korea Data Bank (KDB) correlation (www.infosys.korea.ac.kr/kdb/index.html) was used for literature data. Following is the KDB correlation equation:

$$\ln(Pvp) = A * \ln(T) + \frac{B}{T} + C + D * T^2 \qquad (7.1)$$

Where:

$Pvp =$ Vapour pressure. The parameters A , B , C , D are specific of the pure component.

Table 7-4 provides the constants for ethane and propane as well as the relative deviations.

Table 7-4: Vapour pressure constants from the KDB correlation for ethane and propane and the deviations of the measured vapour-pressure data from the correlation.

	Propane	Ethane
A	-5.395526	-5.381564
B	$-3.383994*10^{03}$	$-2.626728*10^{03}$
C	$4.814260*10^{01}$	$4.639131*10^{01}$
D	$9.132115*10^{-06}$	$1.601858*10^{-05}$
T range (K)	279.24 to 360.17	283.86 to 307.27
% RD	0.21	0.09

RD – Relative deviation

The Relative Deviation was calculated using the equation below:

$$RD = \left(\frac{P_{cor} - P_{\exp}}{P_{cor}} \right) 100 \tag{7.2}$$

Where:

RD : Relative Deviation

P_{cor} : Correlated Pressure

$P_{\exp}$: Experimental Pressure

Table 7-5: Comparison between experimental and correlated vapour-pressure for propane

Temperature (K)	**Pressure Experimental (MPa)**	**Pressure Correlated (MPa)**	**ΔP**	**Deviation %**
279.24	0.5706	0.5713	0.0007	-0.10
283.23	0.6407	0.6409	0.0001	-0.02
288.24	0.7355	0.7361	0.0006	-0.09
293.21	0.8410	0.8413	0.0003	-0.04
298.22	0.9572	0.9577	0.0005	-0.05

Temperature (K)	Pressure Experimental (MPa)	Pressure Correlated (MPa)	ΔP	Deviation %
303.20	1.0843	1.0846	0.0003	-0.03
311.21	1.2820	1.2843	0.0023	-0.20
320.12	1.6038	1.6070	0.0032	-0.20
330.23	1.9924	1.9943	0.0019	-0.10
340.12	2.4301	2.4339	0.0038	-0.20
350.18	2.9530	2.9492	-0.0038	0.10
360.17	3.5400	3.5346	-0.0054	0.20

Table 7-6: Comparison between experimental and correlated vapour-pressure for ethane

Temperature (K)	Pressure Experimental (MPa)	Pressure Correlated (MPa)	ΔP	Deviation %
283.86	3.0867	3.0884	0.0017	0.06
288.80	3.4325	3.4355	0.0030	0.09
293.39	3.7826	3.7803	-0.0023	-0.06
298.61	4.1989	4.1991	0.0002	0.01
303.47	4.6152	4.6150	-0.0002	-0.01

Vapour-pressure measurements were used as preliminary test on the equipment. Only few points were measured for ethane, due to its relative low critical temperature, which is 305.40 K. As detailed above, measured data were compared to literature data (correlated data). Good agreement was observed between data measured in this project and data produced by the KDB correlation, especially for the ethane vapour-pressure, for which the deviation was less than 0.09 %, with a conclusion that the test was successful. The equipment was found suitable to produce accurate vapour-pressure data for pure component.

7.4.2 Vapour-liquid equilibrium measurements

The measured data were regressed on the basis of minimizing the objective function, using the direct method, with the Peng Robinson EOS including the Mathias Copeman alpha function, with the Wong Sandler Mixing Rule incorporating the NRTL activity coefficient model, PR-MC-WS (NRTL).

The experimental data were regressed for the NRTL parameters τ_{ji} and the binary interaction parameter for the WS mixing rule k_{ij}. The α_{ji} parameter for the NRTL is recommended to be set at 0.3 for VLE as stated by Sandler [1997].

The computation was made with the help of THERMOPACK™ software supplied by the Mines Paris Tech. The computational time was of few seconds (around 3 to 5 seconds).

The objective function was calculated from a flash adjustment calculation, below is the equation:

$$F = \frac{100}{N}\left[\sum\left(\frac{x_{\exp} - x_{cal}}{x_{\exp}}\right)^2 + \sum\left(\frac{y_{\exp} - y_{cal}}{y_{\exp}}\right)^2\right] \quad (7.3)$$

7.4.2.1 Test system: R116 + Propane

The R116 (1) + propane (2) system was used to investigate the accuracy and the reliability of the equipment. The reason for the choice of this system was that accurate and duplicated data could be found in literature. Three isotherms were measured and compared to the literature data with an uncertainty of ± 3%. These isotherms were chosen as one below and two above the critical temperature of the least volatile component of the system, which is R116.

The experimental data were correlated with the PR-MC-WS (NRTL). The measured data and the deviation of the correlation are presented in the table below.

Table 7-7: P-x-y data for the R116 (1) + Propane (2) Test system

Pressure / MPa	x_1 / Exp	y_1 / Exp	Δx_1	Δy_1
		T = 291.22 K		
0.793	0.000	0.000	0.000	0.000
0.924	0.015	0.121	0.001	-0.009
1.069	0.033	0.222	0.000	-0.017
1.338	0.076	0.376	0.002	-0.009
1.572	0.122	0.468	0.000	-0.006
1.767	0.171	0.530	-0.003	-0.005
1.891	0.212	0.565	-0.004	-0.003
2.053	0.291	0.613	0.009	0.005
2.194	0.343	0.640	-0.012	-0.003
2.271	0.418	0.672	0.017	0.011
2.386	0.491	0.702	0.012	0.013
2.513	0.567	0.732	-0.012	0.007
3.001	1.000	1.000	0.000	0.000
		T = 296.23 K		
0.905	0.000	0.000	0.000	0.000
1.053	0.016	0.123	0.000	-0.004
1.131	0.024	0.167	-0.001	-0.015
1.324	0.051	0.284	0.000	-0.006

Pressure / MPa	x_1 / Exp	y_1 / Exp	Δx_1	Δy_1
1.502	0.080	0.362	0.001	-0.007
1.804	0.140	0.460	0.001	-0.009
2.036	0.196	0.521	-0.005	-0.009
2.187	0.254	0.564	0.000	0.000
2.751	0.551	0.703	-0.002	0.011
2.857	0.602	0.725	-0.022	0.002
		T = 308.21 K		
1.225	0.000	0.000	0.000	0.000
1.482	0.022	0.122	-0.002	-0.029
1.864	0.076	0.294	0.007	-0.007
2.379	0.161	0.419	-0.001	-0.014
2.650	0.234	0.486	0.000	0.000

With:

$$\Delta x_1 = x_{\text{exp}} - x_{cor}$$

and

$$\Delta y_1 = y_{\text{exp}} - y_{cor}$$

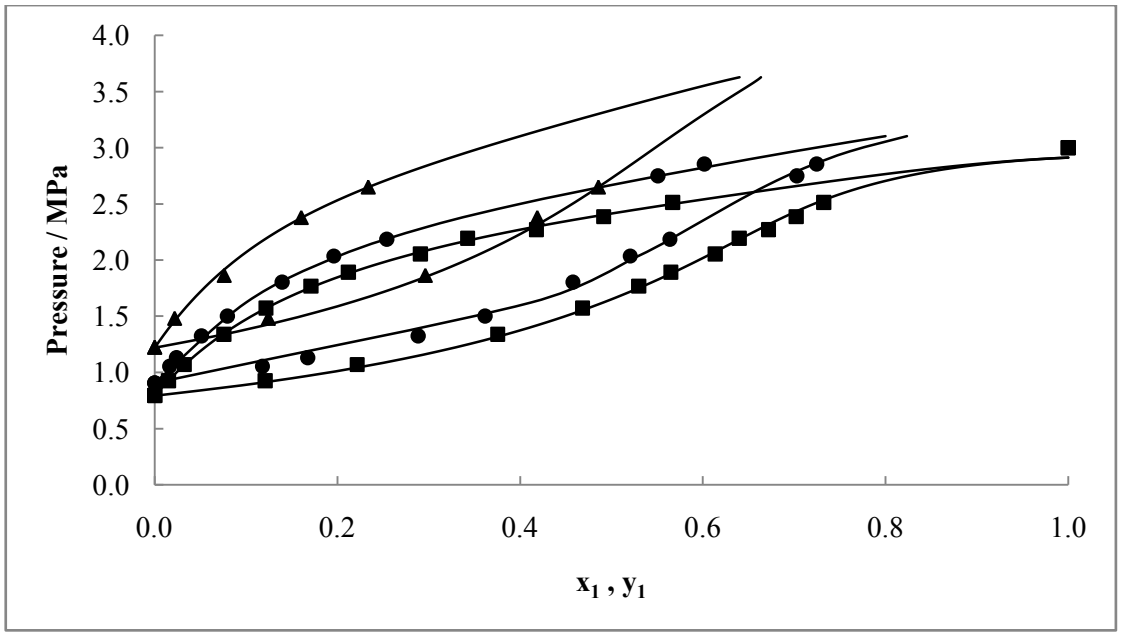

Figure 7-5: Plot of the P-x-y data for the R116 (1) + propane (2) system: ■, 291.22 K; ●, 296.23 K; ▲, 308.21 K; ——, PR-MC-WS (NRTL) model

As observed on the figure 7-5, the correlation fitted well with the measured data for all three isotherms. There is an excellent agreement between the model and the experimental data.
The regressed model parameters and the objective function for the three isotherms are presented in the following table:

Table 7-8: Regressed model parameters for the R116 (1) + Propane (2) system using the PR-MC-WS (NTRL) model ($\alpha = 0.3$)

Parameter	Temperature / K		
	291.22	296.23	308.21
τ_{21} /J.mol^{-1}	-1456	-724	-829
τ_{12} /J.mol^{-1}	5433	4731	5661
k_{ij}	0.37	0.31	0.26
Fobj	4.2	3.6	8.0

Above the critical temperature, the interaction parameters tend to decrease with temperature. The same tendency has been observed with the literature data (Ramjugernath et al. [2009]).
The experimental data for the three isotherms were compared to the data published by Ramjugernath et al. [2009] to evaluate the reproducibility and the reliability of the equipment. The comparison is presented on the following graph.

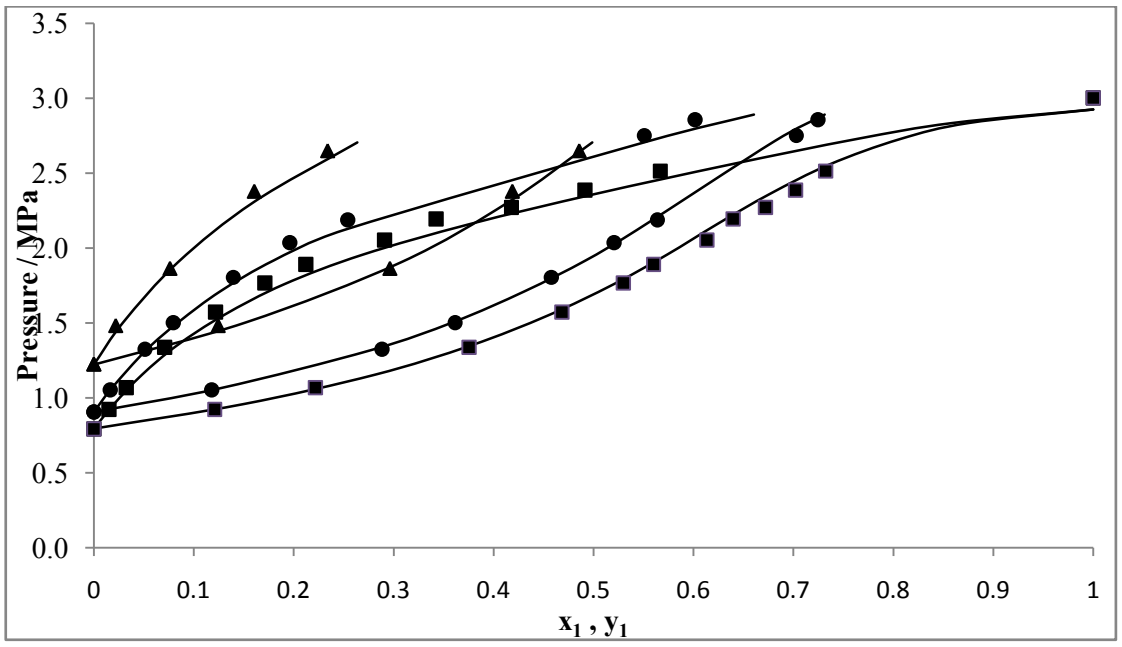

Figure 7-6: Plot of the P-x-y data for the R116 (1) + propane (2) system; ■, 291.22 K; ●, 296.23 K; ▲, 308.21 K; —— Ramjugernath et al. (2009).

The graph shows a good agreement between the literature data (Ramjugernath et al. [2009]) and the experimental data for all three isotherms. The experimental data represented by points are well aligned on the literature data represented by the lines.

Another way of comparing data is by plotting their composition against relative volatility (α), which was calculated via the following equation:

$$\alpha = \frac{y_1 / x_1}{y_2 / x_2} \tag{7.4}$$

This method appears more accurate than the previous since it deals directly with the composition. The comparison is presented on the following graphs for each isotherm.

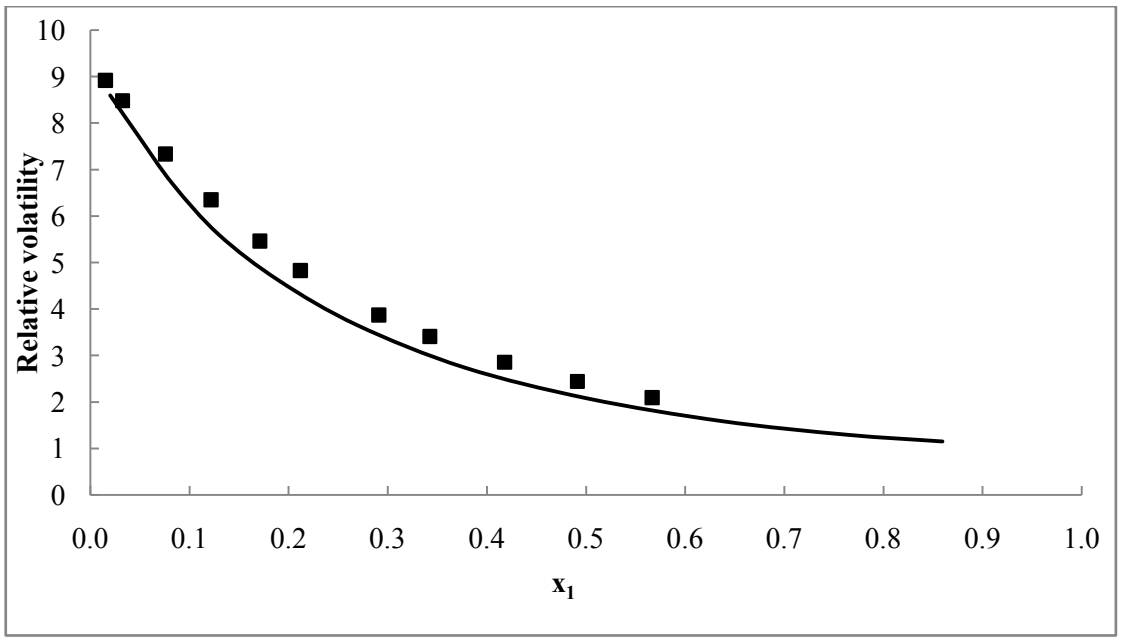

Figure 7-7: Plot of the relative volatility-x_1 data for the R116 (1) + Propane (2) system at 291.22 K: ■, our work; ——, Ramjugernath et al. (2009).

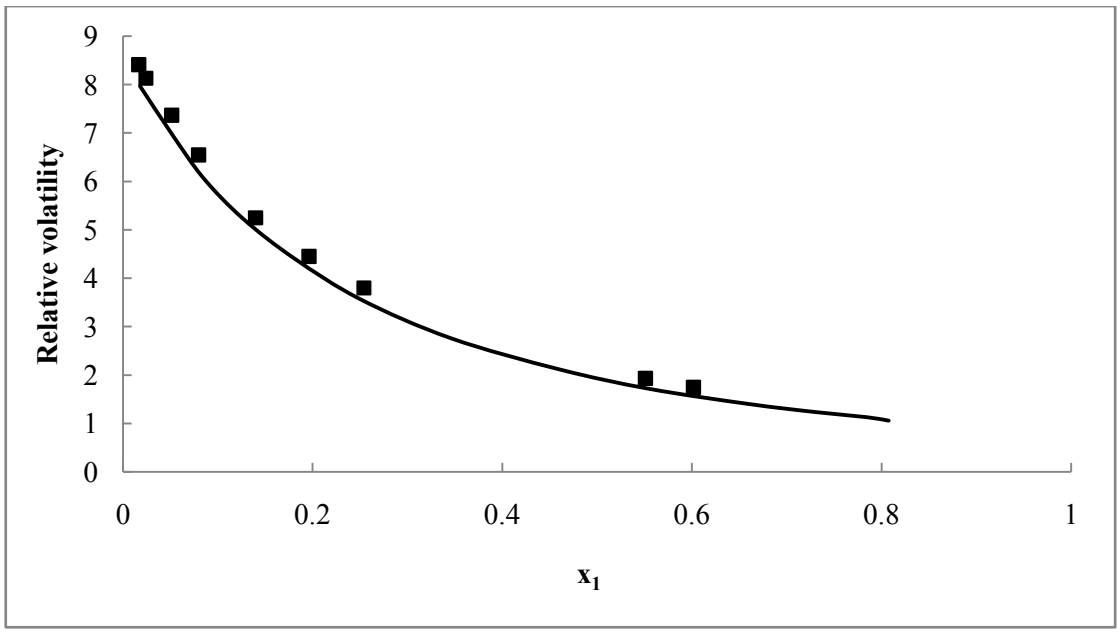

Figure 7-8: Plot of the relative volatility-x_1 data for the R116 (1) + Propane (2) system at 296.23 K:■, our work; ——, Ramjugernath et al. (2009).

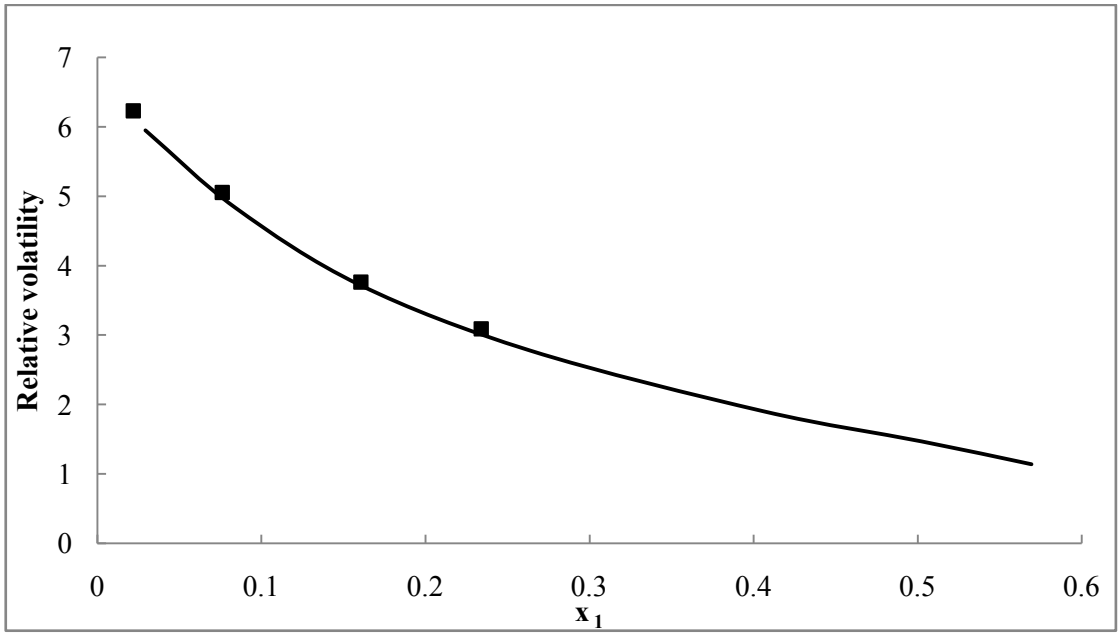

Figure 7-9: Plot of the relative volatility-x_1 data for the R116 (1) + Propane (2) at 308.21 K:■, our work; ——, Ramjugernath et al. (2009).

The numerical deviation between the experimental and literature relative volatility is presented in the following table. The deviation was calculated using the Average Absolute Deviation (equation 7.5).

Table 7-9: Deviations between the experimental and literature Relative deviation

Temperature / K	AAD α
291.22	5.43
296.23	2.52
308.21	2.41

Good agreement has been observed between the data produced in this work and those of Ramjugernath (2009) both graphically and numerically. The relative volatility comparison of both sets of data (this work and Ramjugernath [2009]) was satisfactory, except for the first isotherm (at 291.22 K), where slight discrepancies have been observed, but not enough to discredit the experimental data. From these comparisons, one can say that the test system was well conducted.

In summary, after producing reliable vapour-pressure data and now reliable vapour-liquid equilibrium data, the equipment was considered accurate and suitable for further measurements.

Thermodynamic consistency test

The thermodynamic consistency test was applied to the experimental data to verify the accuracy**.** The Van Ness-Byer-Gibbs test was used. The method consisted of vapour molar fraction. If the average magnitude of the y-residual is less than 0.010, the data are considered thermodynamically consistent (Jackson, 1995). The results of the thermodynamic consistency test for all the isotherms of the R116 (1) + Propane (2) system are presented on the following graph

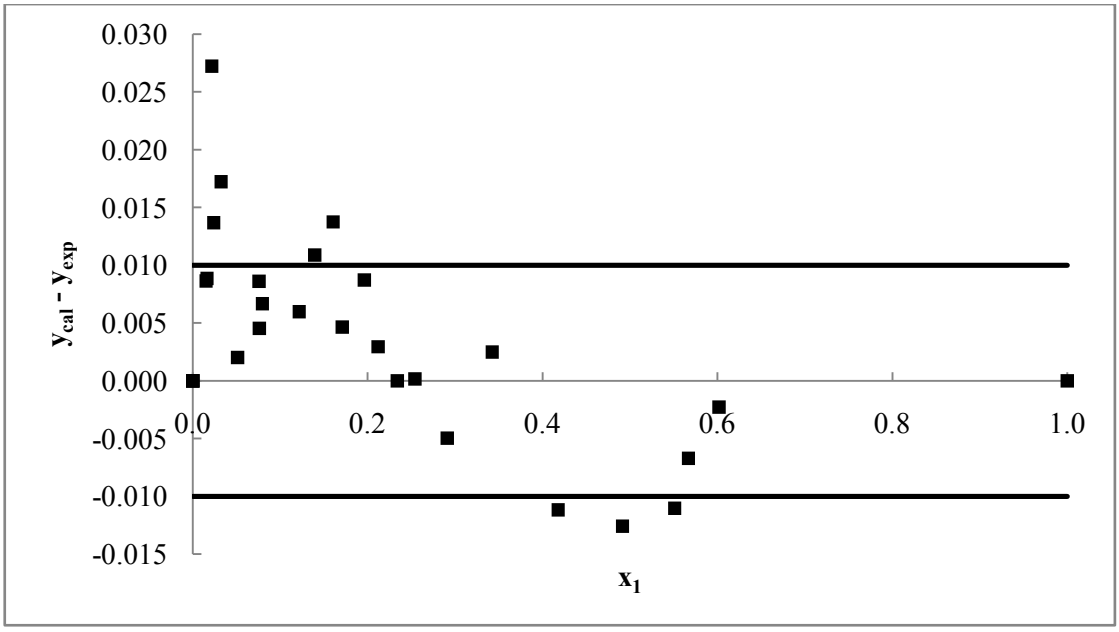

Figure 7-10: Thermodynamic consistency test for the R116 (1) + Propane (2) system

The points are well distributed along the x-axis, the scattering is limited at 0.015 on the y-axis. This can be interpreted that the experimental data are thermodynamically consistent.

7.4.2.2 New system: Ethane + HFPO

The P-x-y data for the Ethane (1) + HFPO (2) system at the various isotherms are presented in Table 7-10 and on Figure 7-10. Five isotherms were measured; three below and two above the critical temperature of ethane, in order to observe the transition of the system at the critical point. The data were measured with an uncertainty on the composition of ± 3 %.

Table 7-10: P-x-y data for the Ethane (1) + HFPO (2) System

Pressure / MPa	x_1	y_1	Pressure / MPa	x_1	y_1
	T = 283.39 K			T = 290.32 K	
0.458	0.000	0.000	0.547	0.000	0.000
0.673	0.044	0.313	1.009	0.104	0.449
0.875	0.110	0.477	1.317	0.191	0.572
1.188	0.210	0.605	1.611	0.290	0.652
1.398	0.275	0.659	1.823	0.349	0.691
1.653	0.361	0.716	2.087	0.436	0.735
1.877	0.433	0.755	2.341	0.515	0.768
2.056	0.493	0.782	2.512	0.573	0.793
2.267	0.574	0.814	2.771	0.670	0.831
2.511	0.678	0.851	2.974	0.739	0.860

Pressure / MPa	x_1	y_1	Pressure / MPa	x_1	y_1
	T = 283.39 K			T = 290.32 K	
2.705	0.749	0.878	3.119	0.792	0.882
2.833	0.830	0.916	3.333	0.879	0.933
2.894	0.870	0.935	3.535	1.000	1.000
3.086	1.000	1.000			
	T = 298.67 K			T = 308.42 K	
0.707	0.000	0.000	0.922	0.000	0.000
1.145	0.092	0.385	1.455	0.097	0.336
1.603	0.210	0.549	1.847	0.187	0.467
1.855	0.276	0.608	2.089	0.241	0.522
2.103	0.338	0.653	2.340	0.304	0.573
2.407	0.422	0.704	2.619	0.372	0.618
2.634	0.493	0.739	2.885	0.432	0.652
2.872	0.560	0.767	3.103	0.481	0.680
3.097	0.629	0.795	3.306	0.529	0.702
3.326	0.696	0.824	3.517	0.577	0.726
3.601	0.792	0.871	3.813	0.652	0.762
3.754	0.836	0.892	4.100	0.720	0.791
4.161	1.000	1.000	4.389	0.795	0.825
	T= 318.45 K				
1.177	0.000	0.000			
1.833	0.126	0.331			
2.117	0.183	0.418			
2.405	0.244	0.478			
2.671	0.294	0.521			
2.969	0.350	0.563			
3.239	0.397	0.594			
3.570	0.463	0.628			
3.881	0.530	0.653			
4.144	0.587	0.672			

The two last isotherms are incomplete. They were limited by the critical point. At the critical point there was formation of a black substance in the cell. The viewer could not distinguish the vapour from the liquid phase.

The P-x-y data for the Ethane (1) + HFPO (2) system are presented graphically on the Figure 7-7, following below:

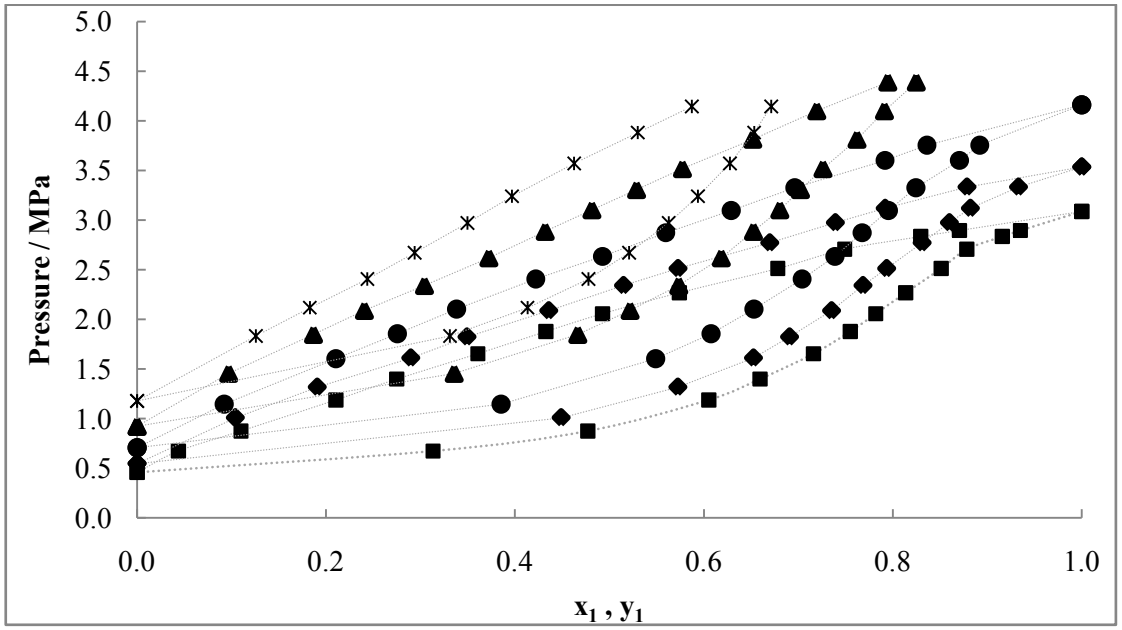

Figure 7-11: Experimental P-x-y data for the Ethane (1) + HFPO (2) system;▮ , 283.39 K; ◆, 290.32 K;● , 298.67 K;▲ ,308.42 K; ✳,318.45 K; ..... , smoothed line

7.4.2.3 Reduction of the experimental data

As said previously, the reduction of the VLE data incorporated the flash calculations based on the direct method. The thermodynamic model involved the PR-MC-WS (NTRL) model. The reduction was done on the basis of minimizing the objective function.

The results of the fitting are graphically presented on the Figure 7-11 and on the Figure 7-12.

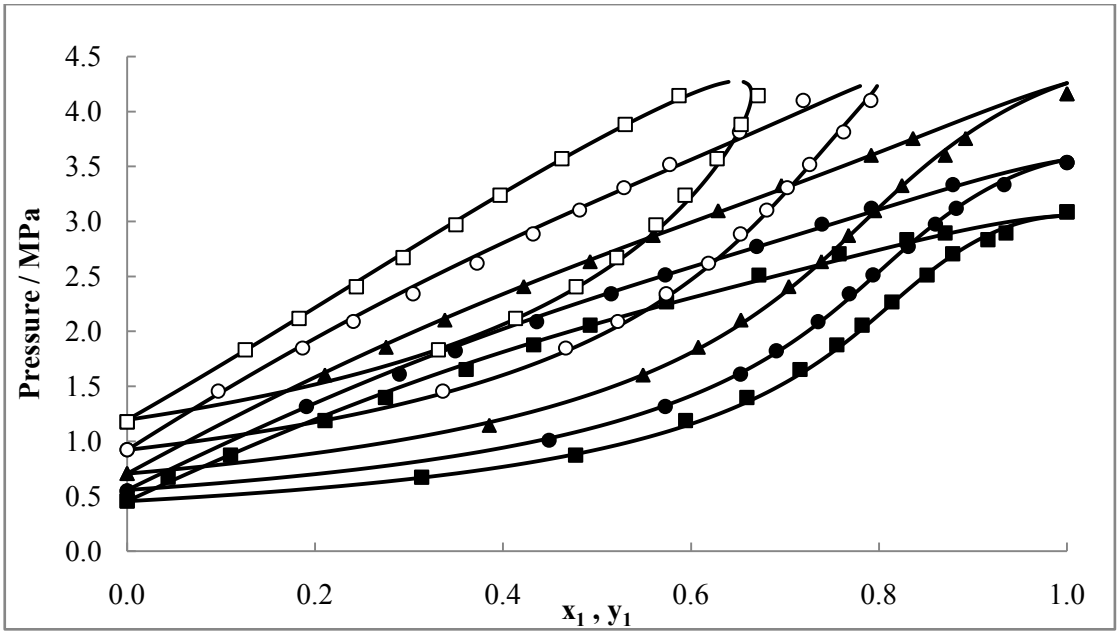

Figure 7-12: Experimental P-x-y data for the Ethane (1) + HFPO (2) system; ■, 283.39 K; ●, 290.32 K; ▲, 298.67 K; ⬭, 308.42 K; □, 318.45 K; ———, PR-MC-WS (NRTL) model

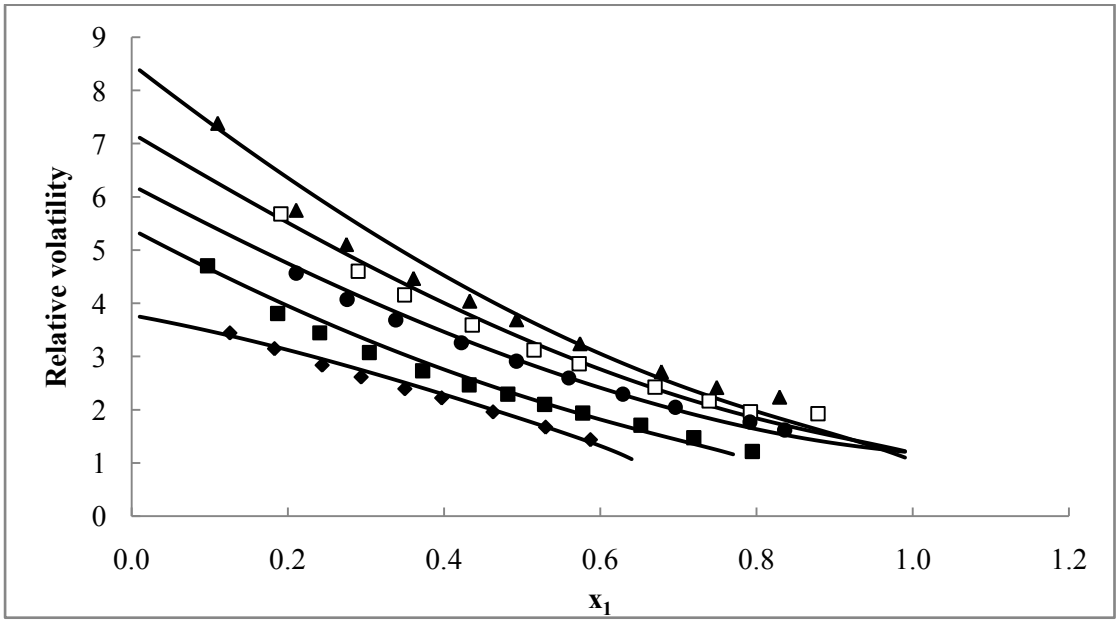

Figure 7-13: Plot of the relative volatility-x_1 data for the Ethane (1) + HFPO (2): ▲, 283.39 K; □, 290.32 K; ⬬, 298.67 K; ■, 308.42 K; ◆, 318.45 K; ——, PR-MC-WS (NRTL) model.

Two representations were used to investigate how well the experimental data and the model match each other. Firstly, the data were plotted on the graph P-x-y, as shown on the Figure 7-8,

the model represented by the line matched the experimental data points closely. Secondly, the data of the relative volatility was plotted against the liquid molar fraction; this representation has the advantage of comparing only the compositions, since the flash calculation was used as objective function. The regression matched the experimental data, except some discrepancies could be observed for the first isotherm (283.39 K). An explanation of this could be found in the fact that the equipment was difficult to stabilize while working at low temperature. At 283.39 K, some fluctuations of the temperature were observed on the equipment. The performance of the refrigeration unit was suspected to be the cause of this problem.

Table 7-10 shows the binary interaction parameters and the NRTL parameters for the five isotherms obtained after fitting the measured data on the basis of minimizing the objective function of equation.

Table 7-11: Regressed model parameters and objective function for the Ethane (1) + HFPO (2) system using the PR-MC-WS (NTRL) model (α = 0.3)

Parameters	**Temperature / K**				
	283.39	290.32	298.67	308.42	318.45
$\tau_{12} / J.mol^{-1}$	8000	6672	5186	5671	10436
$\tau_{21} / J.mol^{-1}$	-280	-625	-664	-538	-1689
k_{ij}	0.13	0.16	0.26	0.19	0.18
Fobj	8.09	4.14	2.65	4.81	2.01

The influence of temperature on the NRTL parameters is presented graphically on the Figure 7-13.

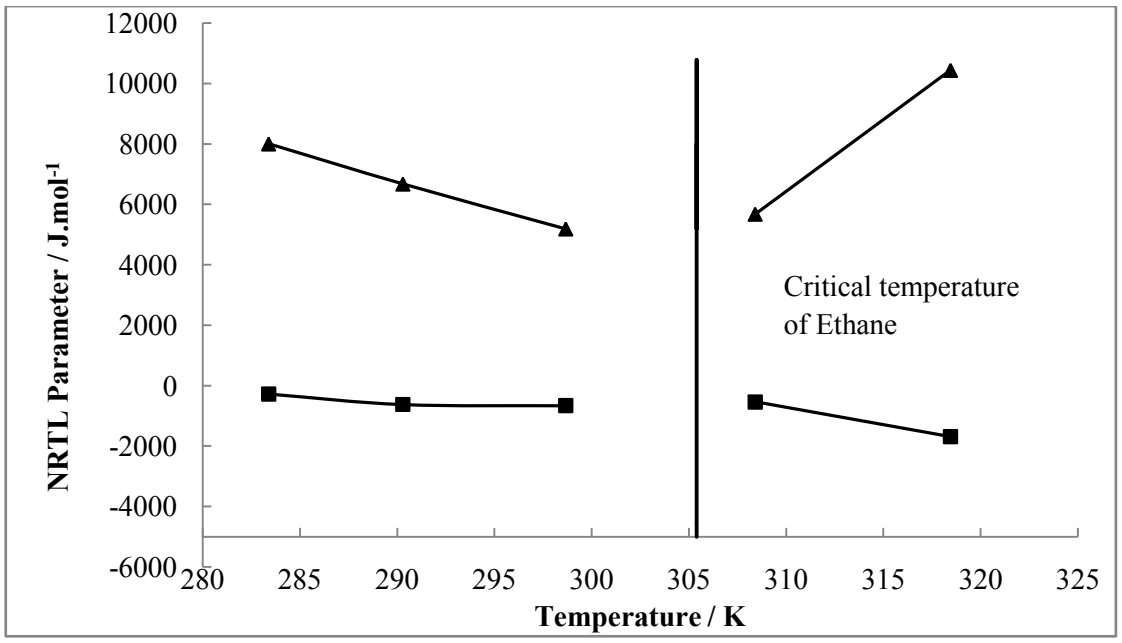

Figure 7-14: Plot of the NRTL temperature dependant parameters; ■ τ_{21}, ▲ τ_{12}.

The influence of temperature on the binary interaction parameter is shown on the following figure:

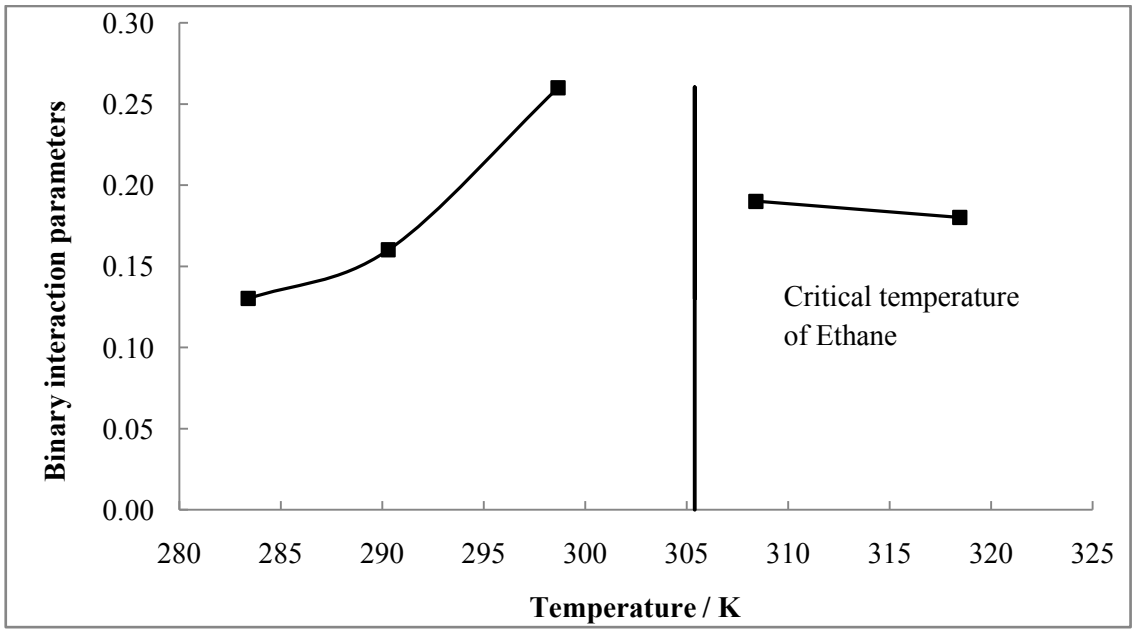

Figure 7-15: Plot of the binary-interaction mixing rule parameter (k_{ij}) dependency with temperature.

The study of the influence of temperature on the NRTL parameter and the binary interaction parameter revealed a discontinuity on the critical temperature of ethane. The tendency of both NRTL and binary interaction parameters changes at the critical point. τ_{12} value decreases below the critical temperature of ethane and increases above that. While τ_{21} value increases below as well as above the critical temperature of ethane, but a discontinuity was observed in the trend at the critical temperature.

For the binary interaction parameter (k_{ij}), the trend increases below the critical temperature of ethane and decreases above that; which is in agreement with the trends of other works on refrigerants system, such as Ramjugernath et al. [2009] on the R116 + propane system, Madani et al. [2008] on the R116 + R134a.

The deviation observed in fitting the experimental data was calculated by the means of the AADU and the BIASU

$$AADU = (100/N)\sum\left|(U_{cal} - U_{\exp})/U_{\exp}\right| \tag{7.5}$$

$$BIASU = (100/N)\sum\left(U_{\exp} - U_{cal}\right)/U_{\exp} \tag{7.6}$$

Table 7-12: Deviations between the experimental data and the model data for the Ethane (1) + HFPO (2) system

Temperature / K	AAD x %	BIAS x %	AAD y %	BIAS y %
283.39	4.4	-1.6	0.8	-0.3
290.32	2.0	0.1	0.5	0.2
298.67	1.4	-0.1	0.7	0.2
308.42	2.9	0.3	1.1	-0.5
318.45	1.3	0.6	0.8	-0.5

For both AADU and BIASU the deviations are less than 4.5%. The highest value of deviation is detected on the first isotherm (283.39 K). As cited previously, minor errors are suspected on the first isotherm, since the equipment had some challenges to stabilize at low temperature. This indicates a good agreement between the experimental data and the correlation.

7.4.2.4 Thermodynamic consistency test

The results of the thermodynamic consistency test for all the isotherms of the Ethane + HFPO system are presented.

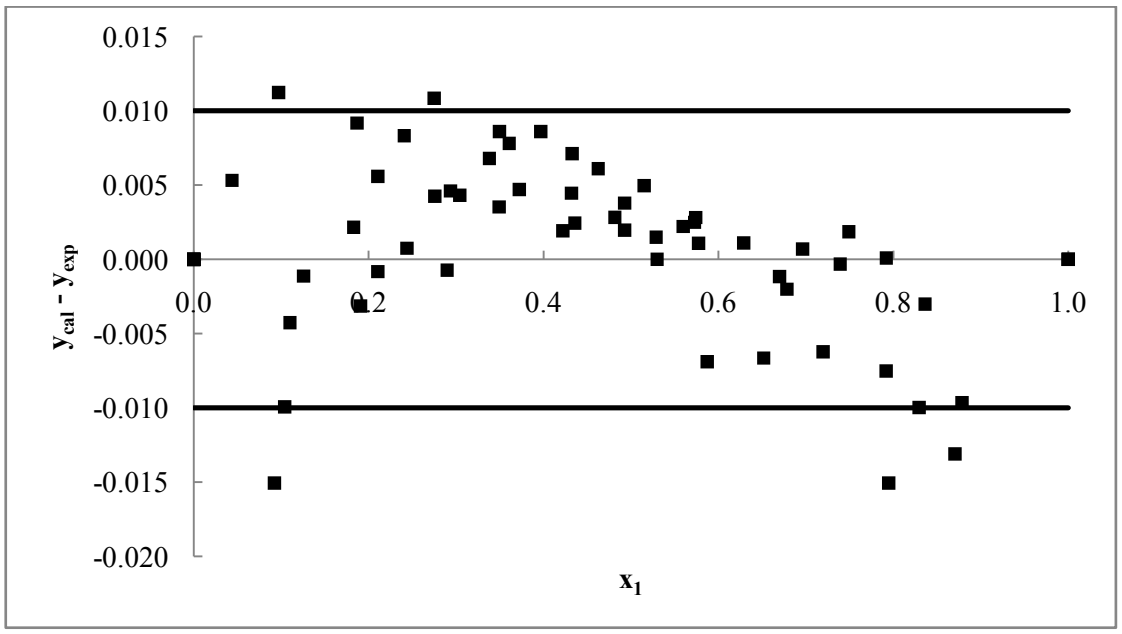

Figure 7-16: Thermodynamic consistency test for the Ethane (1) + HFPO (2) system

From the previous figures, one can see that the points are scattered along the x-axis. The scattering does not exceed 0.015 on the y axis. This implies that the experimental data are thermodynamically consistent.

CHAPTER 8: CONCLUSION

The work undertaken in this study had two aims: (1) the modification of the static HPVLE equipment and (2) the measurement of vapour liquid equilibrium data of fluorinated hydrocarbons.

Concerning the modification, the apparatus designed and constructed by Ramjugernath [2000] and described by Naidoo [2004] was improved. The main modification concerned the sampling method. The previous method was lengthy and had numerous sources of error; this was replaced by the ROLSI^{TM}. The new sampling method was found to be simple and rapid in operation.

The air-bath was redesigned; the actual air-bath was made smaller than the previous, reducing the equilibration time.

A VLE test measurement was performed to verify the accuracy and reliability of the equipment. The R116 + propane system was used as a test system. Three isotherms were measured. The experimental data were found to be in good agreement with those of Ramjugernath et al. [2009]. This led to the conclusion that the equipment was accurate and reliable for further measurements.

High-pressure VLE data of HFPO + ethane were measured. The experimental data were measured at five different temperatures; 283.39 K, 290.32 K, 298.67 K, 308.32 K and 318.45 K. The data were correlated using the direct method, with the Peng-Robinson EOS incorporating the Mathias-Copeman alpha function, with the Wong-Sandler mixing rules and the NRTL activity coefficient model. All the correlations were made with the help of THERMOPACK^{TM} software supplied by the Ecole de Mines, Paris-Tech. The correlation was satisfactory; the deviations between the experimental and the model were in the acceptable range.

The thermodynamic consistency test was done on the experimental data, using the Van-Ness Byer-Gibbs test. The test indicated that the data were consistent.

Hence it is stated that the apparatus described by Naidoo [2004] was improved and the modified apparatus was suitable for HVLE measurements in reasonable time. Accurate HPVLE data

were measured for the system ethane + HFPO, as required for understanding the behaviour of the fluorinated components for multiple purposes.

RECOMMENDATIONS

I. Refrigeration unit

The refrigeration unit included first by Kissun [2001] in this HPVLE apparatus was claimed to help the equipment to perform measurements at temperatures down to 250 K, but it was observed during our work that the lowest temperature that could be reached was approximately 277.15 K and that while going down to temperatures lower than 288.15 K, the temperature fluctuated slightly. This seriously limited the ability of the apparatus; isotherms at low temperature were not measured because of this problem. It is recommended that the refrigeration shall be replaced to return the equipment to its original ability.

II. Future work

Vapour-pressure measurements were performed only for two of the four components comprising the two systems. Vapour-pressure data for HFPO and R116 were not measured as suitable data to which the measured data could be compared, could not be found in literature. We therefore suggest vapour-pressure measurements of these components should be performed in the future. .

Binary VLE measurements for the C_2F_4 + C_2F_6 and the C_3F_6 + C_3F_8, however a supplier could not be found to provide chemicals in the reasonably period of time. It is suggested that for further work these systems be investigated.

LITERATURE CITED

Abrams, D. S. and Prausnitz, J. M., "Statistical Thermodynamics of Liquid Mixtures: A New expression for the Excess Gibbs Energy of Partly or Completely Miscible Systems," *AIChE J.,* **21**, 116-127 (1975)

Alan V. P., Joseph F. and Artulo Jr., "Anaesthetic Properties of a Series of Fluorinated Compound", *Technology and Applied Pharmacology,* **15,** 303-323 (2004)

Ashcroft, S. J., Shearn, R. B. and Williams, C., "A Visual Equilibrium Cell for Multiphase Systems at Pressure up to 690 bar," *Chem. Eng. Res. Des.,* **61**, 51-55 (1983)

Baba-Ahmed, A., Guilbot P. and Richon D., "New Equipment Using a Static-Analytic Method for the Study of Vapour-Liquid Equilibria at Temperatures down to 77 K," *Fluid Phase Equilibria,* 166, 225-236 (1999)

Bae, H. K., Nagahama, K. and Hirata, M., "Measurement and Correlation of High Pressure Vapour-Liquid Equilibria for the systems Ethylene-Propylene," *J. Chem. Eng. Japan,* **14**, 1-6 (1981)

Benedict, M., Webb, G. B. and Rubin, L. C., "An Empirical Equation for Thermodynamic Properties of Light Hydrocarbons and Their Mixtures," *J. Chem. Phys.,* **8,** 334-345 (1940)

Besserer, G. J. and Robinson, D. B., "A High Pressure Autocollimating Refractometer for Determining Coexistence Liquid and Vapour Phase Densities," *Canadian J. Chem. Eng.,* **49,** 651-656 (1971)

Calm, J. M., "The next generation of refrigerants – Historical review, considerations, and outlook" *international journal of refrigeration,* **31,** 1123-1133 (2008)

Chueh, P. L., Muirbrook, N. K. and Prausnitz, J. M., "Part II. Thermodynamic Analysis," *AIChE J.,* **11,** 1097-1102 (1965)

Dahl, S. and Michelsen, M. L., "High Pressure Vapour-liquid Equilibrium with Unifac Based Equation of State," *AIChE.,* **36,** 1829-1836 (1990)

Danner R. P. and Gupte, P. A., "Density Dependent Local Composition Models: An Interpretive Review," *Fluid Phase Equilibria,* **26,** 415-430 (1986)

Deiters, U. K. and Schneider, G. M., "High Pressure Phase Equilibria: Experimental Methods," *Fluid Phase Equilibria*, **29,** 145-160 (1986)

Dohrn, R. and Brunner, G., "High Pressure Fluid-Phase Equilibria: Experimental Methods and Systems Investigated (1988-1993)," *Fluid Phase Equilibria*, **106,** 213-282 (1995)

Durkee J., Ph. D Thesis, *Cleaning for Contamination Control,* P.E. 2002

Dymond, J. H. and Smith, E. B., The *Virial Coefficients of Pure Gases and Mixtures,* Clarendon Press, Oxford (1980)

Figuiere, P., Hom, J., Laugier, S., Renon, H., Richon D. and Szwarc, H., "Vapour-Liquid Equilibria up to 40000 KPa and 400C: a New Static Method," *AIChE J.,* **26,** 872-875 (1980)

Fredenslund, A., Mollerup, J. and Chriatiansen, L., "An apparatus for Accurate Determinations of Vapour-Liquid Equilibrium Properties and Gas PVT Properties," *Cryogenics,* **13,** 414 (1973)

Fredenslund, A., Gmehling, J. and Rasmussen, P., *Vapour-Liquid Equilibria Using UNIFAC,* 1st ed., Elsevier, Amsterdam (1977)

Gess, M. A., Danner, R. P. and Nagvekar, M., "Thermodynamic Analysis of Vapor-Liquid Equilibria: Recommended Models and a Standard Data Base," *Design Institute for Physical Property Data, American Institute for Chemical Engineers* (1991)

Guibot, P. Valtz, A., Legendre, H., Richon, D., "Rapid online sampler-Injector- A reliable Tool for HT-HP sampling and online analysis", *Analysis,* **28,** 426-431 (2000)

Guillevic, J., Richon, D., and Renon, H., "Vapor-Liquid Equilibrium Measurements up to 558 K and 7 MPa: A New Apparatus," *Ind. Eng. Chem. Fund.,* **22,** 495 (1983)

Harmens, A. and Knapp, H., "Three-parameter cubic equation of state for normal substances." Ind. Eng. Chem. Fund., **19,** 291-294 (1980)

Heyen, G., In Neuman, S. (Ed), "A Cubic Equation of State with Extended Range of Application," *Second World Congress on Chemical Engineering*, Montreal, Canada, 41-46 (1981)

Huang, S. S. S., Le, A. D., Ng H. J. and Robinson, D. B., "The Phase Behaviour of Two Mixtures of Methane, Carbon Dioxide, Hydrogen Sulphide and Water," *Fluid Phase Equilibria,* **19,** 21-32 (1985)

Huron, M. J. and Vidal, J., "New Mixing Rules in Simple Equations of State for Representing Vapour-Liquid Equilibria of Strongly Non-ideal Mixtures," *Fluid Phase Equilibria,* **3,** 255-271 (1979)

Inomata, H., Tuchiya, K., Arai, K. and Saito, V., "Measurement of Vapour-Liquid Equilibria at Elevated Temperatures and Pressures Using a Flow Type Apparatus," *J. Chem. Eng. Japan.* **19,** 386 (1986)

Jackson, P. L. and Wilsak, R. A., "Thermodynamic Consistency Tests Based on the Gibbs-Duhem Equation Applied to Isothermal Binary Vapour-Liquid Equilibrium Data: Data Evaluation and Model Testing," *Fluid Phase Equilibria,* **103**, 155-197 (1995)

Kalra, H. and Robinson, D. B. "An Apparatus for the Simultaneous Measurement of Equilibrium Phase Compositions and Refractive Index Data at Low Temperatures and High Pressures," *Cryogenics,* **15,** 409 (1975)

Kalra, H., Kubota, H., Robinson, D. B. and Ng, H. J., "Equilibrium Phase Properties of the Carbon Dioxide-n-Heptane System," *J. Chem. Eng. Data,* **23,** 317-321 (1978)

Kang, Y. W. and Lee, Y. Y., "Vapor-Liquid Equilibria for the Systems Composed of 1-Chloro-1,1-Difluoroethane, 1,1-Dichloro-1-Fluorothane, and 1,1,1-Trichloroethane at 50.1^{o} C " J. Chem. Eng. Data, **41,** 303-305(1996)

Kiplinger, J. L., Richmond, T. G. and Osterberg C. E., "Activation of Carbon-Fluorine Bonds by Metal Complexes," *Chem. Rev.* **94,** 373-431 (1994)

Klink, A. E., Chueh, H. Y. and Amich Jr., "The Vapor-Liquid Equilibrium of the hydrogen-n-Butane System at Elevated Pressures," *AIChE J.,* **21,** 1142-1148 (1975)

Kobayashi, R. and Katz, D. L., "Vapour-Liquid Equilibria for Binary Hydrocarbon-Water Systems," *Ind. Eng. Chem.,* **45,** 440-451 (1953)

Konrad, R., Swaid, I. and Schneider, G., "High-Pressure Phase Studies on Fluid Mixtures of Low-Volatile Organic Substances with Supercritical Carbon Dioxide," *Fluid Phase Equilibria,* **10,** 307 (1983)

Laugier, S. and Richon, D., "New Apparatus to Perform Fast Determinations of Mixture Vapor-Liquid Equilibria up to 10 MPa and 423 K," *fuel,* **62,** 842 (1983)

Legret, D., Richon, D. and Renon, H., "Vapor-Liquid Equilibria up to 100 MPa," *AIChE J.*, **27,** 203-207. (1981)

Lemal, D. M., "Perspective on Fluorocarbon Chemistry," *J. Org. Chem.,* **54,** 123-134 (2004)

Lewandowski G., Meissner, E. and Milchert E., "Special Applications of Fluorinated Organic Compounds," *J. Hazard Mater*, **137**, 385-391 (2006)

Liebermann E., Fried V., "Thermodynamic Consistency Test Methods," *Ind. Eng. Chem. Fundamen,* **11(2)**, 280-281 (1972)

Lin, H. M., Kim, H., Leet, W. A., and Chao, V., "A New Vapour-Liquid Equilibrium Apparatus For Elevated Temperatures and Pressures," *Ind. Eng. Chem. Fundam.,* **24,** 260-262 (1985)

Mahieu et al., "Fluorinated Hydrocarbon Compounds, their use in Cosmetic Compositions, Method of Preparing and Cosmetic Compositions Containing Them," *Patent Storm* **10**, 12-13 (1995)

Malanowski, S., "Experimental Methods for Vapour-Liquid Equilibria: Part 1. Circulation Methods," *Fluid Phase Equilibria,* **8,** 197-219 (1985)

Malanowski, S and Anderko, A., *Modelling Phase Equilibria: Thermodynamic Background and Practical Tools,* John Wiley and Sons Inc., (1992)

Margules, M., S.-B. *Akad. Wiss. Wien, math-naturwiss. KI. II.,* 104,1234 (1895)

Mathias, P. M., and Copeman T. W., "Extension of the Peng-Robinson Equation of State to Complex Mixtures: Evaluation of the Various Forms of the Local Composition Concept," *Fluid Phase Equilibria,* **13,** 91 (1983)

McClean, B., "Worldwide Semiconductor Market to reach $ 400 billion in 2011," *IC. Insights* (2008)

Michael, M. Abbott "Low-Pressure Phase Equilibria: Measurement of VLE". *Fluid Phase Equilibria,* **29,**193-207 (1986)

Mollerup J. and Lundgraad L., "Calculation of Phase Diagrams of gas-hydrates," *Fluid Phase Equilibria,* **76,** 141 (1992)

Moodley, K. "High-pressure Vapour-Liquid Equilibrium studies at Low temperatures", PhD Dissertation, University of Natal, Durban, South Africa (2002)

Mühlbauer, A. L., *Measurement and Thermodynamic interpretation of High-Pressure Vapour-Liquid Equilibrium Data*, PhD Dissertation, University of Natal, Durban, South Africa (1990)

Mühlbauer, A. L. and Raal, J. D., "Measurement and Thermodynamic interpretation of High-Pressure Vapour-Liquid Equilibria in the toluene-CO2 system", *Fluid Phase Equilibria,* **64,** 213-236 (1991)

Mühlbauer, A. L. and Raal, J. D., "Computation and Thermodynamic Interpretation of High Pressure Vapour-Liquid Equilibria- A Review," *Chem. Eng. J.,* **60,** 1-29 (1995)

Naidoo, P., "*High-Pressure Vapour-Liquid Equilibrium studies"*, PhD Dissertation, University of KwaZulu Natal, Durban, South Africa (2004)

Nakayama, T., Sagara, H., Arai, K. and Saito, S., "High Pressure Liquid-Liquid Equilibria for the System of Water, Ethanol and 1,1-Difluoroethane at 323.2 K," *Fluid Phase Equilibria,* **38,** 109-127 (1987)

Ng, H. J. and Robinson, D. B., "Equilibrium Phase Properties of the Toluene-Carbon Dioxide System," *J. Chem. Eng. Data,* **23,** 325 (1978)

O'Hagan D., "Understanding Organofluorine Chemistry, An Introduction to the C-F Bond," *Chem. Sc,* **37,** 308-319 (2008)

Panagiotopoulos, A. Z. and Reid, R. C. Chao, K. and Robinson, R. (Eds), *Equations of State-Theories and Applications,* ACS Symp. Ser. No. 300, American Chemical Society, Washington DC, USA (1986)

Peng, D. Y. and Robinson, D. B., "A New Two-Constant Equation of State," *Ind. Eng. Chem. Fundam.,* **15,** 59-63 (1976)

Prausnitz, J. M., Lichtenthaler, R. N. and de Azevedo, E. G., *Molecular Thermodynamics of Fluid-Phase Equilibria,* 2nd ed., Prentice-Hall, Englewood Cliffs, NJ, USA (1986)

Raal, J. D. and Mühlbauer, A. L., "The measurement of High Pressure Vapour-Liquid Equilibria", *Dev. Chem. Eng. Mineral Process.*, **2,** 69-105 (1994)

Raal, J. D. and Mühlbauer, A. L., *Phase equilibria; Measurement and computation*, Taylor and Francis, Bristol, PA (1998)

Ramjugernath, D., *High pressure Vapour-Liquid equilibrium studies,* PhD Dissertation, university of Kwazulu Natal, Durban, South Africa (2000)

Ramjugernath, D., Valtz, A., Coquelet, C., Richon, D., "Isothermal Vapor-Liquid Equilibrium Data for the Hexafluoroethane (R116) + Propane System at Temperatures from 263 to 323 K," *J. Chem. Eng. Data,* **54,** 1292-1296 (2009)

Redlich, O. and Kwong, J. N. S., "On the Thermodynamics of Solutions: V: An Equation of State. Fugacities of Gaseous Solutions," *Chem. Rev.,* **44,** 233-244 (1949)

Reid, R. C., Prausnitz, J. M. and Poling, B. E. *The Properties of Gases and Liquids*, 4th ed., McGraw-Hill, New York, NY, USA (1987)

Reiff, W., Peters-Gerth P. and Lucas, K., "A Static Equilibrium Apparatus for (Vapor + Liquid) Equilibrium Measurements at High Temperatures and Pressures. Results for (Methane + n-Pentane)," *J. Chem. Thermo.,* **19,** 467-477 (1987)

Renon, H. and Prausnitz, J. M. "Local Compositions in Thermodynamics Excess Functions for Liquid Mixtures," *J. Chem. Thermo.,* **19,** 135-144 (1968)

Rigas, T., Mason, D. and Thodos, G., "Vapor-Liquid Equilibria. Microsampling Technique Applied to a New Variable Volume Cell," *Ind. Eng. Chem.,* **50,** 1297 (1958)

Rogers, B. L. and Prausnitz, J. M., "Sample-Extrusion Apparatus for High Pressure Vapor-Liquid Equilibria: Compositions and Densities at Pressures up to the Critical," Ind. *Eng. Chem Fundam.,* **9,** 174-177 (1970)

S. A. B. Viera de Melo, P.Pallado, G. B. Guarise and A. Bertucoo " High-Pressure Vapour-Liquid equilibrium Data for binary and ternary systems

formed by supercritical CO2, LIMONENE AND LINALOOL". *Braz. J. Chem. Eng.,***16,** 1 (1999)

Sagara, H., Arai, Y. and Saito, S., "Vapor-Liquid Equilibria of Binary and Ternary Systems Containing Hydrogen and Light Hydrocarbons," *J. Chem. Eng.* Japan, **5,** 339-348 (1972)

Sandler, S. I., Orbey, H. and Lee, B.-I., *Models for thermodynamic and Phase equilibria calculations,* Marcel-Dekkert, New York, NY, USA (1994)

Sandler, S. I, *Chemical and Engineering Thermodynamics (Third edition),* New York, John Wiley & Sons, Inc. (1997)

Schmidt, G. and Wenzel, H., "A modified van der Waals equation of state" *Chem. Eng. Sci.*, **35,** 1503-1512 (1980)

Shibata, S. K. and Sandler, S. I., "High-Pressure Vapor-Liquid Equilibria Involving Mixtures of Nitrogen, Carbon Dioxide and n-Butane," *J. Chem. Eng. Data*, **34,** 291-298 (1989)

Shimawaki, Fuji, K., and Higashi, Y., "Precise measurements of the Vapour-Liquid equilibria (VLE) of HFC-32/134a mixtures using a new apparatus. *International journal of Thermodynamics*, **23,** 801-808. (2002)

Simnick, J. J., Lawson, C. C., Lin, H. M. and Chao, K. C. "Vapor-Liquid Equilibrium of Hydrogen/Tetralin System at Elevated Temperatures and Pressures," *AIChe. J.,* **23,** 469-476 (1977)

Smith, J. M., Van ness, H. C and Abbott, M. M., *Introduction to chemical Engineering Thermodynamics, 7th edition,* McGraw Hill international Edition, Chemical Engineering Series, Singapore (2005)

Soave, G., "Equilibrium Constants from a Modified Redlich-Kwong Equation of State," *Chem. Eng. Sci.,* **27,** 1197-1203 (1972)

Soave, G., "Application of a cubic equation of state to vapour-liquid equilibria of systems containing polar compounds," *Inst. Chem. Eng. Symp.Ser.,* **56,** 1.2/1-1.2/16 (1979)

Stein, F. P., stener, C. J and Geist, J. M "Vapour-Liquid equilibrium apparatus for cryogenic systems", *Chem. Eng. Progr.,* **58,** 70-73 (1962)

Stryjek, R. and Vera, J. H. "PRSV: An Improved Peng-Robinson Equation of State for Pure Compounds and Mixtures," *Canadian J. Chem. Eng.,* **64,** 323-333 (1981)

Swaid, PhD Thesis, *Calculation of Fluid-fluid and Solid-fluid Phase Equilibria in Binary Mixtures at High Pressures,* University of Bochum (1984)

Tinoco, Sauer, *Wang and Puglisi, Physical Chemistry,* Prentice Hall (2002)

Tsonopoulos, C. and Heidman, J. L. "High Pressure Vapour-Liquid Equilibria with Cubic Equations of State," *Fluid Phase Equilibria,* **29,** 391-414 (1986)

Tsuboka T. and Katayama T., "Modified Wilson equation for vapor-liquid and liquid-liquid equilibria," *J. Chem, Eng. Jpn.,* **8,** 181-187 (1975)

Valtz A., Coquelet C., Baba-Ahmed A. and Richon D., "Vapour-Liquid Equilibrium Data for the Propane (R227ea) System at Temperatures from 293.16 to 353.18 K and Pressures up to 3.4 MPa," *Fluid Phase Equilibria,* **202,** 24-47 (2002)

Van der Waals, J. H., *On the Continuity of the Gaseous and Liquid State*, Doctoral Dissertation, Leiden (1873)

Van Laar, J. J., "The Vapor Pressure of Binary Mixtures," *Z. Physik. Chem.,* **72,** 723-751 (1910)

Van Laar, J. J., "On the Theory of Vapor Pressures of Binary Mixtures," *Z. Physik. Chem.,* **83,** 599-608 (1913)

Van Ness, H. C., Byers, S. M and Gibbs, R. E., "Vapour-Liquid equilibrium: part1. An apparatus of Data Reduction Methods" *AIChE J.,* **19,** 238-244 (1973)

Vetere, A. "A Simple Modification of the NRTL Equation," *Fluid Phase Equilibria,* **173,** 57-64 (2000)

Wagner, Z. and Wichterle, I., "High Pressure Vapour-Liquid Equilibrium in systems Containing Carbon Dioxide, 1-Hexene, and n-Hexane," *Fluid Phase Equilibria,* **33,** 109-123 (1987)

Walas, S.M., *Phase equilibria in chemical engineering,* Butterworth, Boston, MA, USA (1985)

Wichterle, I., "High-Pressure Vapour-Liquid Equilibria. IV-quantitative Description. Part 2," *Fluid Phase equilibria,* **2,** 59-78 (1978a)

Wichterle, I., "High-Pressure Vapour-Liquid Equilibria. V-Quantitative Description. Part 3," *Fluid Phase equilibria,* **2,** 143-159. (1978b)

Wilson, G. M., "Vapor-Liquid Equilibrium. XI: A New Expression for the Excess Free Energy of Mixing," *J. Am. Chem. Soc.,* **86,** 127-130 (1964)

Wilson and Gisvold, *Anaesthetic,* Wow Essays, Dream Net, Boston, USA (2004)

Won K. W. and Prausnitz, J. M., "High-Pressure vapour-Liquid equilibria calculation of Partial pressures from total pressure data. Thermodynamic consistency", Ind. Eng. *Chem. Fudam.*, **12,** 459-463 (1973)

Wong, D. S. H., and Sandler, S. I., "A Theoretically Correct Mixing Rule for Cubic Equations of State," *AiChE J.,* **38,** 671-680 (1992)

www.history.nasa.gov/conghand/propelnt.html (20th January 2010)

www.Infosys.Korea.ac.kr/kdb/index.html (14th December 2009)

Xu, N., Yao, J., Wang, Y., Shi, J. and Lu, B. C. Y.,"Vapor-Liquid Equilibria of Five Binary Systems Containing R-22," *Fluid Phase Equilibria,* **69,** 261-270 (1991)

Zabaloy, M. S., Mabe, G. D. B., Bottini, S. B. and Brignole, E. A. "Isothermal Vapor-Liquid Equilibrium Data for Binaries Propane-2-Propanol and Propylene-2-Propanol," *J. Chem. Eng. Data,* **38,** 40-43 (1993)

APPENDIX A

Nomenclature of Fluorinated Hydrocarbons

Generally fluorinated hydrocarbons are classified in four principal nomenclature systems. These four systems are the International Union of Pure and Applied Chemistry (IUPAC), the Chemical Abstract System (CAS), the "Per" system and the "H" system.

The IUPAC and the CAS systems are the same and preferred by many scientists for long time; this system uses a conventional Latin or Greek numeral root to indicate the number of fluorine atoms in the organic compound.

The "per" system denotes substitution of all hydrogen bonded to the carbon by the fluorine atoms.

The "H" system related to polyfluorinated compounds comprising hydrogen atoms less than four. And the hydrogen/fluorine ratio is less than 1:3. The name comprised the number of fluorine atoms and the position of hydrogen in the molecule.

The following table gives examples of different nomenclature systems.

Table A.1: Comparison of Acceptable Nomenclature Systems for Fluorine Compounds (Kirk-Othmer, 1966).

Compound	IUPAC	CAS	Per	H
$CF_3CF_2CF_2$	Octafluoro propane	Octafluoro propane	Perfluoro propane	
$CF_3CH_2CF_3$	1,1,1,3,3,3-hexa-fluoropropane	1,1,1,3,3,3-hexa-fluoropropane		2H,2H-hexa-fluoro propane
CF_3COOH	Trifluoethanoic acid	Trifluoroacetic acid	Perfluoacetic acid	

Compound	IUPAC	CAS	Per	H
CF_3CH_2COOH	3,3,3-trifluoro propanoic acid	2,2,2-trifluoro-propionic acid		2H,2H-trifluoro-propionic acid
$CF_3CF_2CF_2OCF_2CF_2CF_3$	Heptafluoro propoxy-heptafluoroprop ane	Bis(heptafluoro-propyl) ether	Perfluoro-propyl ether	

The chemical names of fluorinated hydrocarbons were judged weighty in the refrigerant field. A simple system was developed by DuPont concerning fluorinated hydrocarbons used as refrigerants. The system consisted on indentifying different element by the numbers. The numbering system rules are presenting like this:

Moving from the right:

1. The first digit is the number of fluorine (F) atoms.
2. The second digit is the number of hydrogen (H) atoms plus one.
3. The third digit is the number of carbon (C) atoms minus one. When this digit is zero it is omitted from the number.
4. The fourth digit is the number of unsaturated carbon-carbon bonds. When this digit is zero it is omitted from the number.

Example:

R116

Where:

R: means refrigerant
1: means there are 1+1= 2 carbon atoms
1: means there is 1-1= 0 hydrogen atom
6: means there are 6 fluorine atoms

APPENDIX B

GC Calibrations

The calibration of TCD for all four components comprised in the two systems involved in this work was performed by the direct injection method. Samples were injected to the GC by the means of gas syringe. Known volumes of the component were injected repeatedly. This led to relation number of moles peak areas.

B.1 Propane calibration

Known volumes of propane were injected into the GC with the means of gas syringe. The injections were in the range of 50 µl to 1 ml. Attention was paid to take an accurate volume. The number of moles of gas injected was calculated from the ideal gas equation.

$$n = \frac{PV}{RT} \tag{B.1}$$

The sample was taken at atmospheric pressure, P was measured using a barometer. T is the temperature of the withdrawn sample (the room temperature) measured by the means of a thermometer. R is the gas constant. V is the withdrawn volume.

$P = 100340$ Pa
$T = 296.15$ K
$R = 8.314$ m^3 Pa mol^{-1} K^{-1}

The different calculations needed in the calibration are presented in the following table.

Table B.1: Propane GC Calibration results (n is the number of moles obtained from the ideal gas equation, calculated n is the number of moles obtained using the calibration equation, deviation is the relative deviation between the number of moles).

VOLUME INJECTED / µl	PEAK AREA	PEAK AREA SQUARE	n	CALCULATED n	DEVIATION
1000	15862102	2.51606E+14	4.07523E-05	4.10377E-05	0.700160593
1000	15930073	2.53767E+14	4.07523E-05	4.12025E-05	1.104661908
1000	15414101	2.37595E+14	4.07523E-05	3.99487E-05	-1.972067924
1000	15616914	2.43888E+14	4.07523E-05	4.04422E-05	-0.761009671
1000	15742183	2.47816E+14	4.07523E-05	4.07466E-05	-0.014083143
800	12831787	1.64655E+14	3.26019E-05	3.35869E-05	3.021357177
800	12312600	1.516E+14	3.26019E-05	3.22904E-05	-0.95541649
800	12266412	1.50465E+14	3.26019E-05	3.21747E-05	-1.310071126
800	12815333	1.64233E+14	3.26019E-05	3.35459E-05	2.895603502
800	12315634	1.51675E+14	3.26019E-05	3.2298E-05	-0.932129784
600	9045008	8.18122E+13	2.44514E-05	2.39966E-05	-1.85987455
600	9034986	8.1631E+13	2.44514E-05	2.39708E-05	-1.965357505
600	9144172	8.36159E+13	2.44514E-05	2.42517E-05	-0.816587988
600	9211311	8.48483E+13	2.44514E-05	2.44243E-05	-0.110723351
600	9147541	8.36775E+13	2.44514E-05	2.42604E-05	-0.781154402
400	6170311	3.80727E+13	1.63009E-05	1.65089E-05	1.276034376
400	6136953	3.76622E+13	1.63009E-05	1.6421E-05	0.736573743
400	6149403	3.78152E+13	1.63009E-05	1.64538E-05	0.93792371
400	6176117	3.81444E+13	1.63009E-05	1.65242E-05	1.369915224
400	6111089	3.73454E+13	1.63009E-05	1.63528E-05	0.318192628
200	3082739	9.50328E+12	8.15046E-06	8.26744E-06	1.435162605
200	3083315	9.50683E+12	8.15046E-06	8.26899E-06	1.454269254
200	3084148	9.51197E+12	8.15046E-06	8.27124E-06	1.481884539
200	3081180	9.49367E+12	8.15046E-06	8.26322E-06	1.383486006
200	3084148	9.51197E+12	8.15046E-06	8.27124E-06	1.481884539
100	1529373	2.33898E+12	4.07523E-06	4.04306E-06	-0.789475107
100	1542288	2.37866E+12	4.07523E-06	4.0784E-06	0.077699935
100	1542814	2.38028E+12	4.07523E-06	4.07984E-06	0.112974295
100	1526343	2.32972E+12	4.07523E-06	4.03477E-06	-0.992927225
100	1510288	2.28097E+12	4.07523E-06	3.99083E-06	-2.070995987
50	772937	5.97432E+11	2.03762E-06	1.96701E-06	-3.464967238
50	772323	5.96483E+11	2.03762E-06	1.96532E-06	-3.547901738
50	774281	5.99512E+11	2.03762E-06	1.97071E-06	-3.283401658
50	776343	6.02709E+11	2.03762E-06	1.97639E-06	-3.004842723
50	771288	5.94887E+11	2.03762E-06	1.96248E-06	-3.687657881

The deviation was obtained using the following equation:

$$D = \left(\frac{n_{cal} - n}{n} \right) 100 \tag{B.2}$$

Where:

D : Deviation

n_{cal} : calculated number of moles

n : number of moles

A second order polynomial equation was produced combining the peak area and the number of moles. The Linest function of Microsoft Excel 2007 was used to produce the equation. Following is the equation:

$$n = -1.0828 * 10^{-28} A^2 + 2.7694 * 10^{-12} A - 1.671 * 10^{-01} \tag{B.3}$$

The same procedure was applied for all components and polynomial equations were provided in the Chapter VI.

APPENDIX C

Properties of compounds considered in this work

C.1 Introduction

This work involved the following components, propane, R116, HFPO, ethane. Some of the properties of these compounds are presented below:

C.2 Physical and thermodynamic properties

Table C.2: Physical and thermodynamics properties from DDB. HFPO properties were obtained from DuPont

Component	M g/mol	T_f / K	T_b / K	T_c / K	P_c / bar	V_c cm^3/mol	Z_c	ω
Propane	44.09	85.45	231.02	369.95	42.46	203.0	0.2802	0.1520
R116	138.01	172.40	194.88	293.03	30.42	221.9	0.2771	0.2290
HFPO*	166.00	129.15	246.15	358.93	31.36	-	0.2723	0.3529
Ethane	30.07	89.85	184.48	305.40	48.83	148.0	0.2847	0.0980

C.3 Mathias Copeman Coefficients using the PR EOS

Table C.3: Mathias Copeman coefficients obtained from THERMOPACK^{TM} software.

COEFFICIENTS	Propane	R116	HFPO*	Ethane
c_1	0.6001	0.7963	1.1122	0.5313
c_2	-0.0063	-0.5512	-2.3146	-0.0618
c_3	0.1739	0.1032	3.1430	0.2142

***** Values obtained from fitting of experimental vapour pressure data.